Effects of heat transfer on MHD suction–injection model of viscous fluid flow through Differential transformation and Hermite wavelet techniques

K. R. Raghunatha[1], Vinod Y.[1], and Kumbinarasaiah S.[2*]

[1]Department of Mathematics, Davangere University, Davangere- 577 007, India

[2*]Department of Mathematics, Bangalore University, Bangalore- 560056, India

Corresponding author email: kumbinarasiah@gmail.com

Abstract.

This study investigates the magnetohydrodynamic flow and heat transfer between two parallel disks, considering suction and injection effects at the disks. The governing equations describing the flow and thermal transport are derived based on the principles of mass, momentum and energy conservation for an electrically conducting fluid. As the governing partial differential equations (PDEs) are highly nonlinear, similarity transformations are applied to transform them into coupled ordinary differential equations (ODEs). Numerical techniques, namely the Hermite wavelet method (HWM) and Differential transformation technique (DTT) are then employed to solve the transformed equations. Parametric effects of several influential parameters such as the Prandtl number, squeeze number, Hartmann number, and thermophoresis parameter on the velocity and temperature profiles are systematically analyzed. Comparisons are made with previous findings in the literature. The results indicate significant dependence of flow behavior and heat transfer on the governing parameters. Velocity and temperature distributions in the boundary layer are presented and discussed in detail. The proposed mathematical model and numerical approach provide useful insights into heat transfer characteristics for parallel disk systems and similar engineering applications involving magnetohydrodynamic flows with suction or injection effects.

Keywords Heat transfer, MHD, Viscous fluid, Hermite wavelet method, Differential transformation method.

1. Introduction

Mathematical modeling of various phenomena in diverse fields such as engineering, science and technology often involves nonlinear differential equations. Such nonlinear equations naturally arise in many real-world problems in fluid dynamics, materials science, biology and other domains[1-3]. However, analytical solutions are rarely feasible for most nonlinear problems except in trivial cases. As a result, numerical methods are commonly employed to

obtain approximate solutions. In recent years, several numerical techniques have been proposed for solving highly nonlinear differential equations, including the Runge-Kutta method, homotopy perturbation method, finite difference approaches, optimal homotopy analysis and numerical wavelet approaches. In particular, the HWM [4] and DTT have gained prominence due to their accuracy and effectiveness in handling nonlinear terms. This study focuses on applying the above methods to solve nonlinear differential equations modeling important engineering and scientific phenomena. The ability of these numerical techniques to provide solutions is systematically evaluated for various nonlinear problems.

The DTT is a semi-analytical technique that requires only a few parameters. It produces a polynomial-like solution for the given equation. In contrast to the traditional Taylor series approach, the DTT does not demand high computational resources for solving highly nonlinear problems without linearization or discretization [5-7]. Previous studies have effectively applied this method to solve various fluid flow problems. Numerical wavelet methods have gained significant attention in recent years for solving differential equations arising in diverse fields such as signal processing, image analysis and mathematical modeling. Notable contributions include the use of Laguerre wavelets [8], Taylor wavelets [9], cardinal B-splines [10], Bernoulli wavelets [11] and Hermite wavelets [12, 13]. Among these, the HWM has been widely utilized due to its accuracy. Given the effectiveness of numerical wavelet techniques, developing a parametric Hermite wavelet approach for nonlinear problems is important. With the availability of powerful computational software, HWM has been successfully employed by researchers to solve various nonlinear boundary value problems, including different fluid flow models [14-21]. This study aims to apply the HWM to analyze the present magnetohydrodynamic flow problem.

The study of viscous fluid flows involves fundamental fluid mechanics principles to analyze complex real-world flows. Most problems exhibit nonlinear and turbulent behaviors. Past work by researchers like Leal [22] has provided insights into viscosity and particle motion within fluids. Viscous fluids have important applications, for example as brake oil which helps reduce motion in hydraulic brakes. Fluid viscosity also impacts blood flow through arteries and veins. Significant research efforts like those by MacCormack [23] have developed numerical techniques to model equations governing compressible viscous flows. Recent studies by authors such as Jalili et al. [24] and Zhang et al [25] have analyzed viscous fluid flow and heat transfer between permeable disks as well as nonlinear convection effects on such flows. This has enhanced my understanding of complex flow dynamics and viscosity.

The present study similarly aims to apply numerical methods to model magnetohydrodynamic viscous flow between parallel disks, in line with past efforts to analyze industrial and biomedical applications involving viscous fluids.

Due to the no-slip condition at fluid-solid boundaries, velocity decreases near walls. To control this, either fluid can be injected through porous surfaces or suctioned away to smooth velocity profiles. Suction extracts fluid impacted by no-slip, drawing it towards walls. Injection enhances velocities by adding more fluid. Past studies have analyzed suction effects. Zaturska et al. [26] examined suction in porous channel flows. Attia [27] investigated unsteady flows between plates under suction and injection. Mahmood [28] used homotopy methods for a deformable channel with wall suction/injection in porous media. Yuan and Finkelstein [29] explained laminar pipe flows through porous walls with injection/suction. Abdollahi et al. [30] analyzed heat transfer between parallel surfaces under hybrid nanofluid suction/injection using numerical techniques. These findings provide useful insights into controlling boundary layer development through suction/injection in viscous flows. The present study similarly considers these effects in the modeled magnetohydrodynamic problem.

Heat transfer [31, 32] concept plays a significant role across various fields including engineering and technology. Convection involves the transfer of heat via molecular interchange as hot and cold fluids move at different temperatures, such as when a surface contacts a flowing fluid. Previous studies have provided useful insights. Ahmad et al. [33] analyzed heat transfer and time-dependent viscous flows, employing finite difference methods to obtain profiles considering Hartmann and Eckert numbers. Zukauskas [34] examined forced convective heat transfer in viscous flows, focusing on the viscous sublayer disturbance. Ismail [35] numerically studied viscous fluid behaviors in mini-channel heat exchangers. Rosenberg and Hellums [36] investigated developing flows and heat transfer for varying viscosity fluids. Bathe and Dong [37] used software to solve incompressible viscous flows with heat transfer.

Magnetohydrodynamics (MHD) examines the motion of electrically conducting fluids under magnetic fields, important in plasmas, liquid metals, salt water and electrolytes [38-42]. MHD has applications in spacecraft propulsion, astrophysics and more. Previous studies provide useful insights. Sa'adaldin and Qatanani[43] analytically and numerically examined unsteady MHD flows. Nesliturk and Tezer-Sezgin[44] studied high Hartmann number MHD

flows using finite elements. More recently, Guled et al. [45] analyzed heat transfer effects on MHD slip flow over shrinking sheets using optimal homotopy methods. Akbar et al. [46] examined heat transfer for MHD viscous fluids in ciliated tubes. Shah et al. [47] studied MHD and porous effects on free convection between plates. Bhargavi et al. [48] analyzed conjugate heat transfer for MHD viscous flow past permeable plates. Raghunatha et al [49] examined heat transfer effects on MHD suction–injection viscous flows using numerical techniques.

To the best of our knowledge, applications of the DTM and HWM to magnetohydrodynamic (MHD) suction-injection viscous fluid flow problems have not been reported in previous literature. This study aims to solve the highly nonlinear governing equations using DTM and HWM. The implementation of these numerical techniques was discussed in our past works [18, 49]. The impact of influential physical parameters such as the Prandtl number, squeeze number, Hartmann number, suction/blowing parameter and thermophoresis parameter on the velocity and temperature distributions in the boundary layer are examined. The paper is organized as follows: Section 2 formulates the problem. Sections 3 and 4 present the basics and methodology of DTM and HWM, respectively. Section 5 discusses the results and Section 6 provides the conclusions.

2. Formulation of the problem

The physical outline is shown in Fig. 1. We study the MHD flow of an incompressible viscous fluid among two parallel infinite disks, generated by a distance, $h(t) = H\sqrt{1-\alpha t}$ .Additionally, if $\alpha > 0$ causes the plates to pinch together until they touch at $t = \frac{1}{\alpha}$, but $\alpha < 0$ causes plates to bear a receding and dilating motion. The lower and upper disks are maintained at constant temperatures $T = T_w$ and $T = T_H$, where T_w is the surface temperature at the lower disk and T_H is the surface temperature at the upper disk. We have selected the cylindrical coordinate arrangement. The rotational symmetry of the flow $\left(\frac{\partial}{\partial \theta} = 0\right)$ and also take the azimuthal velocity component (v) is equal to zero. A uniform magnetic field of strength $B(t) = \frac{B_0}{\sqrt{1-\alpha t}}$ is applied perpendicular to the disks. The nonlinear governing equations for the unsteady 2D axisymmetric flow of a viscous fluid are as follows [50]

$$\frac{\partial u}{\partial r}+\frac{u}{r}+\frac{\partial w}{\partial z}=0, \tag{1}$$

$$\frac{\partial u}{\partial t}+u\frac{\partial u}{\partial r}+w\frac{\partial u}{\partial z}=-\frac{1}{\rho}\frac{\partial p}{\partial r}+\frac{\mu}{\rho}\left(\frac{\partial^2 u}{\partial r^2}+\frac{\partial^2 u}{\partial z^2}+\frac{1}{r}\frac{\partial u}{\partial r}-\frac{u}{r^2}\right)-\frac{\sigma B^2}{\rho^2}u, \tag{2}$$

$$\frac{\partial w}{\partial t}+u\frac{\partial w}{\partial r}+w\frac{\partial w}{\partial z}=-\frac{1}{\rho}\frac{\partial p}{\partial z}+\frac{\mu}{\rho}\left(\frac{\partial^2 w}{\partial r^2}+\frac{\partial^2 w}{\partial z^2}+\frac{1}{r}\frac{\partial w}{\partial r}\right), \tag{3}$$

$$\frac{\partial T}{\partial t}+u\frac{\partial T}{\partial r}+w\frac{\partial T}{\partial z}=\frac{k_f}{\left(\rho c_p\right)_f}\left(\frac{\partial^2 T}{\partial r^2}+\frac{\partial^2 T}{\partial z^2}+\frac{1}{r}\frac{\partial T}{\partial r}\right)+\frac{D_T}{T_m}\left(\left(\frac{\partial T}{\partial r}\right)^2+\left(\frac{\partial T}{\partial z}\right)^2\right). \tag{4}$$

Where u and w are radial and axial velocities along r and z direction, ρ is the density of the fluid, T is the temperature, c_p is the specific heat at constant pressure, μ is the Dynamic viscosity, D_T is the thermophoretic diffusion coefficient, k_f is the thermal conductivity of the fluid and T_m is the mean fluid temperature.

The appropriate boundary conditions for the problem are [50]

$$T=T_H \quad u=0, \quad w=\frac{dh}{dt} \quad \text{at} \quad z=h(t) \quad \text{and} \quad T=T_w \quad u=0, \quad w=\frac{-w_0}{\sqrt{1-\alpha t}} \quad \text{at} \quad z=0. \tag{5}$$

Let us introduce the following similarity quantities

$$\eta=\frac{z}{H(1-\alpha t)^{\frac{1}{2}}},\ u=\frac{\alpha r}{2(1-\alpha t)}\frac{df(\eta)}{d\eta},\ w=\frac{-\alpha H}{(1-\alpha t)^{\frac{1}{2}}}f(\eta),\ \theta=\frac{T-T_H}{T_w-T_H}. \tag{6}$$

After inserting the aforementioned quantities into equations (1) to (4), we detached the pressure gradient from the attained equations.

$$\frac{d^4 f(\eta)}{d\eta^4}-S\left(\eta\frac{d^3 f(\eta)}{d\eta^3}+3\frac{d^2 f(\eta)}{d\eta^2}-2f\frac{d^3 f(\eta)}{d\eta^3}\right)-M^2\frac{d^2 f(\eta)}{d\eta^2}=0, \tag{7}$$

$$\frac{d^2\theta(\eta)}{d\eta^2}+Pr\,S\left(2f\frac{d\theta(\eta)}{d\eta}-\eta\frac{d\theta(\eta)}{d\eta}\right)+Pr\,Nt\left(\frac{d\theta(\eta)}{d\eta}\right)^2=0. \tag{8}$$

The equivalent boundary conditions are

$$f(0)=A,\ \frac{df(0)}{d\eta}=0,\ \ f(1)=0.5,\ \frac{df(1)}{d\eta}=0,\ \theta(0)=1,\ \ \theta(1)=0. \tag{9}$$

Where $S = \frac{\alpha\ H^2}{2\nu_f}$ is the Squeeze number, $Pr = \frac{\nu_f}{\alpha}$ is the Prandtl number, $M = \frac{\sigma B_0{}^2 H^2}{\nu}$ is the Hartmann number, $A = \frac{w_0}{\alpha H}$ is the suction/blowing parameter, and $Nt = \frac{D_T (T_w - T_H)}{\nu T_m}$ is the thermophoresis parameter.

3. The basics of differential transformation method and Hermite wavelet method

3.1 Basics of DTM

The DTM was first introduced by Zhou [51] for solving linear and nonlinear problems in electrical circuit analysis, where it was compared with other techniques. DTM generates an analytical solution in the form of a polynomial set based on the concept of Taylor series. The fundamental principles of DTM have been described in previous works [52, 53] as follows:

DTM works on the assumption that the dependent variable $y(x)$ in the given differential equation is an analytic function within its domain Ω. The solution $y(x)$ is approximated by a polynomial series centred around a point $x = x_i$, which lies within the domain D. This polynomial series takes the form of a Taylor series expansion of $y(x)$ about the point $x = x_i$.

$$y(x) = \sum_{k=0}^{\infty} \frac{(x - x_i)^k}{k!} \left[\frac{d^k y(x)}{dx^k} \right]_{x=x_i} \quad \forall x \in \Omega. \tag{10}$$

In particular, $x_i = 0$ then overhead equation becomes

$$y(x) = \sum_{k=0}^{\infty} \frac{x^k}{k!} \left[\frac{d^k y(x)}{dx^k} \right]_{x=0} \quad \forall x \in \Omega. \tag{11}$$

The differential alteration of the solution $y(x)$ is written as:

$$Y(k) = \sum_{k=0}^{\infty} \frac{\mathrm{N}^k}{k!} \left[\frac{d^k y(x)}{dx^k} \right]_{x=0}, \tag{12}$$

where new solution $y(x)$ and altered solution $Y(k)$. The differential spectrum of $Y(k)$ is limited inside the distance $x \in [0, \mathrm{N}]$ and as well as N is some constant. The differential inverse renovate of $Y(k)$ is well-defined as follows:

$$y(x) = \sum_{k=0}^{\infty} \left(\frac{x}{\mathrm{N}} \right)^k Y(k). \tag{13}$$

The solution $y(x)$ is expressed by a finite power series, and the overhead equation can also be articulated as:

$$y(x) = \sum_{k=0}^{j} \left(\frac{x}{\mathrm{N}} \right)^k Y(k). \tag{14}$$

The basic procedures of DTM are

Novel function	Renovated function
$y(x) = ay_1(x) \pm by_2(x)$	$Y(k) = aY_1(k) \pm bY_2(k)$
$y(x) = \frac{dy_1(x)}{dx}$	$Y(k) = (k+1)\, Y_1(k+1)$
$y(x) = \frac{d^2 y_1(x)}{dx^2}$	$Y(k) = (k+1)(k+2)\, Y_1(k+2)$
$y(x) = y_1(x) y_2(x)$	$Y(k) = \sum_{l=0}^{k} Y_1(l) Y_2(k-l)$
$y(x) = x^r$	$Y(k) = \delta(k-r) = \begin{cases} 0 & r \neq k \\ 1 & r = k \end{cases}$
$y(x) = [y_1(x)]^r$	$Y^r(k) = Y^{r-1}(k) \otimes Y(k) = \sum_{l=0}^{k} Y^{r-1}(l) Y(k-l)$

3.2 | Basics of HWM

Hermite wavelets are well-defined as [12, 13],

$$\phi_{n.m}(x)=\begin{cases}\dfrac{2^{\frac{k-1}{2}}}{\sqrt{\pi}}H_m\left(2^k x-2n+1\right), & \dfrac{n-1}{2^{k-1}}\le x\le\dfrac{n}{2^{k-1}}\\ 0 & \text{elsewhere}\end{cases}. \tag{15}$$

Where $n=1,2,3,...,2^{k-1}$ and $m=0,1,2,3,...,M-1$ and $k\in N$. Here $H_m(x)$ represents Hermite polynomials of degree m with regards to weight function $W(x)=\sqrt{1-x^2}$ on the real line R and pleases the succeeding recurrence formula $H_0(x)=1, H_1(x)=2x,$ $H_{m+2}(x)=2xH_{m+1}(x)-2(m+1)H_m(x)$ where, $m=0,1,2,3,\cdots$.

For a specified nonlinear differential equation, we approximated to the solution as $y(x)$ with the assistance of HWM as follows

$$y(x)=\sum_{n=1}^{\infty}\sum_{m=0}^{\infty}C_{n,m}\phi_{n,m}(x). \tag{16}$$

We estimated $y(x)$ by truncating the series as follows

$$y(x)\approx\sum_{n=1}^{2^{k-1}}\sum_{m=0}^{M-1}C_{n,m}\phi_{n,m}(x)=A^T\phi(x), \tag{17}$$

where A and $\phi(x)$ are $2^{k-1}M\times 1$ matrix,

$$A^T=[C_{1,0},\ldots C_{1,M-1},C_{2,0}\ldots C_{2,M-1},\ldots C_{2^{k-1},0},\ldots C_{2^{k-1},M-1}],$$

$$\phi(x)=[\phi_{1,0},\ldots\phi_{1,M-1},\phi_{2,0},\ldots\phi_{2,M-1},\ldots\phi_{2^{k-1},0},\ldots\phi_{2^{k-1},M-1}]^T.$$

Process of Integration of Matrix

The following are some of the Hermite wavelet basis at $k=1$

$$\phi_{1,0}(x)=\frac{2}{\sqrt{\pi}},$$

$$\phi_{1,1}(x)=\frac{1}{\sqrt{\pi}}(8x-4),$$

$$\phi_{1,2}(x)=\frac{1}{\sqrt{\pi}}(32x^2-32x+4),$$

$$\phi_{1,3}(x)=\frac{1}{\sqrt{\pi}}(128x^3-192x^2+48x+8),$$

$$\phi_{1,4}(x)=\frac{1}{\sqrt{\pi}}(512x^4-1024x^3+384x^2+128x-40),$$

$$\phi_{1,5}(x)=\frac{1}{\sqrt{\pi}}(2048x^5-5120x^4+2560x^3+1280x^2-800x+16),$$

$$\phi_{1,6}(x)=\frac{1}{\sqrt{\pi}}(8192x^6-24576x^5+15360x^4+10240x^3-9600x^2+384x+368),$$

$$\phi_{1,7}(x)=\frac{1}{\sqrt{\pi}}(32768x^7-114688x^6+86016x^5+71680x^4-89600x^3+5376x^2+10304x-928),$$

$$\phi_{1,8}(x)=\frac{1}{\sqrt{\pi}}(131072x^8-524288x^7+458752x^6+458752x^5-716800x^4+57344x^3+164864x^2-29696x-3296),$$

$$\phi_{1,9}(x)=\frac{1}{\sqrt{\pi}}(524288x^9-2359296x^8+2359296x^7+2752512x^6-5160960x^5+516096x^4+1978368x^3-534528x^2-118656x+21440),$$

$$\phi_{1,10}(x)=\frac{1}{\sqrt{\pi}}(2097152x^{10}-10485760x^9+11796480x^8+15728640x^7-34406400x^6+4128768x^5+19783680x^4-7127040x^3-2373120x^2+857600x+16448),$$

$$\phi_{1,11}(x)=\frac{1}{\sqrt{\pi}}(8388608x^{11}-46137344x^{10}+57671680x^9+86507520x^8-216268800x^7+30277632x^6+174096384x^5-78397440x^4-34805760x^3+18867200x^2+723712x-461696),$$

$$\phi_{1,12}(x)=\frac{1}{\sqrt{\pi}}(33554432x^{12}-201326592x^{11}+276824064x^{10}+461373440x^9-1297612800x^8+207618048x^7+1392771072x^6-752615424x^5-417669120x^4+301875200x^3+17369088x^2-22161408x+561536),$$

Where, $\phi_9(x)=[\phi_{1,0}(x),\phi_{1,1}(x),\phi_{1,2}(x),\ \phi_{1,3}(x),\ \phi_{1,4}(x),\ \phi_{1,5}(x),\ \phi_{1,6}(x),\phi_{1,7}(x),\phi_{1,8}(x)]^T$.

Apply the integration regarding with x and limits from 0 to x the above nine bases and explicit it as a linear combination of Hermite wavelet basis as follows.

$$\int_0^x \phi_{1,0}(x) = \left[\frac{1}{2} \quad \frac{1}{4} \quad 0 \quad 0 \quad 0 \quad 0 \quad 0 \quad 0 \quad 0\right] \phi_9(x),$$

$$\int_0^x \phi_{1,1}(x) = \left[\frac{-1}{4} \quad 0 \quad \frac{1}{8} \quad 0 \quad 0 \quad 0 \quad 0 \quad 0 \quad 0\right] \phi_9(x),$$

$$\int_0^x \phi_{1,2}(x) = \left[\frac{-1}{3} \quad 0 \quad 0 \quad \frac{1}{12} \quad 0 \quad 0 \quad 0 \quad 0 \quad 0\right] \phi_9(x),$$

$$\int_0^x \phi_{1,3}(x) = \left[\frac{5}{4} \quad 0 \quad 0 \quad 0 \quad \frac{1}{16} \quad 0 \quad 0 \quad 0 \quad 0\right] \phi_9(x),$$

$$\int_0^x \phi_{1,4}(x) = \left[\frac{-2}{5} \quad 0 \quad 0 \quad 0 \quad 0 \quad \frac{1}{20} \quad 0 \quad 0 \quad 0\right] \phi_9(x),$$

$$\int_0^x \phi_{1,5}(x) = \left[\frac{-23}{3} \quad 0 \quad 0 \quad 0 \quad 0 \quad 0 \quad \frac{1}{24} \quad 0 \quad 0\right] \phi_9(x),$$

$$\int_0^x \phi_{1,6}(x) = \left[\frac{116}{7} \quad 0 \quad 0 \quad 0 \quad 0 \quad 0 \quad 0 \quad \frac{1}{28} \quad 0\right] \phi_9(x),$$

$$\int_0^x \phi_{1,7}(x) = \left[\frac{103}{2} \quad 0 \quad 0 \quad 0 \quad 0 \quad 0 \quad 0 \quad 0 \quad \frac{1}{32}\right] \phi_9(x),$$

$$\int_0^x \phi_{1,8}(x) = \left[\frac{-2680}{9} \quad 0 \quad 0 \quad 0 \quad 0 \quad 0 \quad 0 \quad 0 \quad 0\right] \phi_9(x) + \frac{1}{36}\phi_{1,9}(x).$$

Hence,

$$\int_0^x \phi(x)\,dx = H_{9\times 9}\ \phi_9(x) + \bar{\phi}_9(x),$$

where

$$H_{9\times 9} = \begin{bmatrix} \frac{1}{2} & \frac{1}{4} & 0 & 0 & 0 & 0 & 0 & 0 & 0 \\ \frac{-1}{4} & 0 & \frac{1}{8} & 0 & 0 & 0 & 0 & 0 & 0 \\ \frac{-1}{3} & 0 & 0 & \frac{1}{12} & 0 & 0 & 0 & 0 & 0 \\ \frac{5}{4} & 0 & 0 & 0 & \frac{1}{16} & 0 & 0 & 0 & 0 \\ \frac{-2}{5} & 0 & 0 & 0 & 0 & \frac{1}{20} & 0 & 0 & 0 \\ \frac{-23}{3} & 0 & 0 & 0 & 0 & 0 & \frac{1}{24} & 0 & 0 \\ \frac{116}{7} & 0 & 0 & 0 & 0 & 0 & 0 & \frac{1}{28} & 0 \\ \frac{103}{2} & 0 & 0 & 0 & 0 & 0 & 0 & 0 & \frac{1}{32} \\ \frac{-2680}{9} & 0 & 0 & 0 & 0 & 0 & 0 & 0 & 0 \end{bmatrix}, \quad \bar{\phi}_9(x) = \begin{bmatrix} 0 \\ 0 \\ 0 \\ 0 \\ 0 \\ 0 \\ 0 \\ 0 \\ \frac{1}{36}\phi_{1,9}(x) \end{bmatrix}.$$

Implement the integration to the above nine bases is as follows

$$\int_0^x \int_0^x \phi_{1,0}(x)\,dxdx = \left[\frac{3}{16} \quad \frac{1}{8} \quad \frac{1}{32} \quad 0 \quad 0 \quad 0 \quad 0 \quad 0 \quad 0\right]\phi_9(x),$$

$$\int_0^x \int_0^x \phi_{1,1}(x)\,dxdx = \left[\frac{-1}{6} \quad \frac{-1}{16} \quad 0 \quad \frac{1}{96} \quad 0 \quad 0 \quad 0 \quad 0 \quad 0\right]\phi_9(x),$$

$$\int_0^x \int_0^x \phi_{1,2}(x)\,dxdx = \left[\frac{-1}{16} \quad \frac{-1}{12} \quad 0 \quad 0 \quad \frac{1}{192} \quad 0 \quad 0 \quad 0 \quad 0\right]\phi_9(x),$$

$$\int_0^x \int_0^x \phi_{1,3}(x)\,dxdx = \left[\frac{3}{5} \quad \frac{5}{16} \quad 0 \quad 0 \quad 0 \quad \frac{1}{320} \quad 0 \quad 0 \quad 0\right]\phi_9(x),$$

$$\int_0^x \int_0^x \phi_{1,4}(x)\,dxdx = \left[\frac{-7}{12} \quad \frac{-1}{10} \quad 0 \quad 0 \quad 0 \quad 0 \quad \frac{1}{480} \quad 0 \quad 0\right]\phi_9(x),$$

$$\int_0^x \int_0^x \phi_{1,5}(x)\,dxdx = \left[\frac{-22}{7} \quad \frac{-23}{12} \quad 0 \quad 0 \quad 0 \quad 0 \quad 0 \quad \frac{1}{672} \quad 0\right]\phi_9(x),$$

$$\int_0^x \int_0^x \phi_{1,6}(x)\,dxdx = \left[\frac{81}{8} \quad \frac{29}{7} \quad 0 \quad 0 \quad 0 \quad 0 \quad 0 \quad 0 \quad \frac{1}{896}\right]\phi_9(x),$$

$$\int_0^x \int_0^x \phi_{1,7}(x)\,dxdx = \left[\frac{148}{9} \quad \frac{103}{8} \quad 0 \quad 0 \quad 0 \quad 0 \quad 0 \quad 0 \quad 0\right]\phi_9(x) + \frac{1}{1152}\phi_{1,9}(x),$$

$$\int_0^x \int_0^x \phi_{1,8}(x)\,dxdx = \left[\frac{-773}{5} \quad \frac{-670}{9} \quad 0 \quad 0 \quad 0 \quad 0 \quad 0 \quad 0 \quad 0\right]\phi_9(x) + \frac{1}{1440}\phi_{1,10}(x).$$

Hence,

$$\int_0^x \int_0^x \phi(x)\,dx\,dx = H'_{9\times 9}\ \phi_9(x) + \bar{\phi}'_9(x),$$

where

$$H'_{9\times 9}=\begin{bmatrix} \frac{3}{16} & \frac{1}{8} & \frac{1}{32} & 0 & 0 & 0 & 0 & 0 & 0 \\ \frac{-1}{6} & \frac{-1}{16} & 0 & \frac{1}{96} & 0 & 0 & 0 & 0 & 0 \\ \frac{-1}{16} & \frac{-1}{12} & 0 & 0 & \frac{1}{192} & 0 & 0 & 0 & 0 \\ \frac{3}{5} & \frac{5}{16} & 0 & 0 & 0 & \frac{1}{320} & 0 & 0 & 0 \\ \frac{-7}{12} & \frac{-1}{10} & 0 & 0 & 0 & 0 & \frac{1}{480} & 0 & 0 \\ \frac{-22}{7} & \frac{-23}{12} & 0 & 0 & 0 & 0 & 0 & \frac{1}{672} & 0 \\ \frac{81}{8} & \frac{29}{7} & 0 & 0 & 0 & 0 & 0 & 0 & \frac{1}{896} \\ \frac{148}{9} & \frac{103}{8} & 0 & 0 & 0 & 0 & 0 & 0 & 0 \\ \frac{-773}{5} & \frac{-670}{9} & 0 & 0 & 0 & 0 & 0 & 0 & 0 \end{bmatrix}, \overline{\phi'_9}(x)=\begin{bmatrix} 0 \\ 0 \\ 0 \\ 0 \\ 0 \\ 0 \\ 0 \\ \frac{1}{1152}\phi_{1,9}(x) \\ \frac{1}{1440}\phi_{1,10}(x) \end{bmatrix}.$$

Againemploy the integration to the above nine bases is as follows

$$\int_0^x\int_0^x\int_0^x \phi_{1,0}(x)\,dxdxdx=\left[\frac{5}{96}\quad\frac{3}{64}\quad\frac{1}{64}\quad\frac{1}{384}\quad 0\quad 0\quad 0\quad 0\quad 0\right]\phi_9(x),$$

$$\int_0^x\int_0^x\int_0^x \phi_{1,1}(x)\,dxdxdx=\left[\frac{-7}{128}\quad\frac{-1}{24}\quad\frac{-1}{128}\quad 0\quad\frac{1}{1536}\quad 0\quad 0\quad 0\quad 0\right]\phi_9(x),$$

$$\int_0^x\int_0^x\int_0^x \phi_{1,2}(x)\,dxdxdx=\left[\frac{-1}{80}\quad\frac{-1}{64}\quad\frac{-1}{96}\quad 0\quad 0\quad\frac{1}{3840}\quad 0\quad 0\quad 0\right]\phi_9(x),$$

$$\int_0^x\int_0^x\int_0^x \phi_{1,3}(x)\,dxdxdx=\left[\frac{19}{96}\quad\frac{3}{20}\quad\frac{5}{128}\quad 0\quad 0\quad 0\quad\frac{1}{7680}\quad 0\quad 0\right]\phi_9(x),$$

$$\int_0^x\int_0^x\int_0^x \phi_{1,4}(x)\,dxdxdx=\left[\frac{-13}{56}\quad\frac{-7}{48}\quad\frac{-1}{80}\quad 0\quad 0\quad 0\quad 0\quad\frac{1}{13440}\quad 0\right]\phi_9(x),$$

$$\int_0^x\int_0^x\int_0^x \phi_{1,5}(x)\,dxdxdx=\left[\frac{-65}{64}\quad\frac{-11}{14}\quad\frac{-23}{96}\quad 0\quad 0\quad 0\quad 0\quad 0\quad\frac{1}{21504}\right]\phi_9(x),$$

$$\int_0^x\int_0^x\int_0^x \phi_{1,6}(x)\,dxdxdx=\left[\frac{133}{36}\quad\frac{81}{32}\quad\frac{29}{56}\quad 0\quad 0\quad 0\quad 0\quad 0\quad 0\right]\phi_9(x)+\frac{1}{32256}\phi_{1,9}(x),$$

$$\int_0^x\int_0^x\int_0^x \phi_{1,7}(x)\,dxdxdx=\left[\frac{193}{40}\quad\frac{37}{9}\quad\frac{103}{64}\quad 0\quad 0\quad 0\quad 0\quad 0\quad 0\right]\phi_9(x)+\frac{1}{46080}\phi_{1,10}(x),$$

$$\int_0^x\int_0^x\int_0^x \phi_{1,8}(x)\,dxdxdx=\left[\frac{-1211}{22}\quad\frac{-773}{20}\quad\frac{-335}{36}\quad 0\quad 0\quad 0\quad 0\quad 0\quad 0\right]\phi_9(x)+\frac{1}{63360}\phi_{1,11}(x).$$

Hence,

$$\int_0^x\int_0^x\int_0^x \phi(x)\,dxdxdx = H''_{9\times 9}\ \phi_9(x) + \bar{\phi}''_9(x),$$

where

$$H''_{9\times 9} = \begin{bmatrix} \frac{5}{96} & \frac{3}{64} & \frac{1}{64} & \frac{1}{384} & 0 & 0 & 0 & 0 & 0 \\ \frac{-7}{128} & \frac{-1}{24} & \frac{-1}{128} & 0 & \frac{1}{1536} & 0 & 0 & 0 & 0 \\ \frac{-1}{80} & \frac{-1}{64} & \frac{-1}{96} & 0 & 0 & \frac{1}{3840} & 0 & 0 & 0 \\ \frac{19}{96} & \frac{3}{20} & \frac{5}{128} & 0 & 0 & 0 & \frac{1}{7680} & 0 & 0 \\ \frac{-13}{56} & \frac{-7}{48} & \frac{-1}{80} & 0 & 0 & 0 & 0 & \frac{1}{13440} & 0 \\ \frac{-65}{64} & \frac{-11}{14} & \frac{-23}{96} & 0 & 0 & 0 & 0 & 0 & \frac{1}{21504} \\ \frac{133}{36} & \frac{81}{32} & \frac{29}{56} & 0 & 0 & 0 & 0 & 0 & 0 \\ \frac{193}{40} & \frac{37}{9} & \frac{103}{64} & 0 & 0 & 0 & 0 & 0 & 0 \\ \frac{-1211}{22} & \frac{-773}{20} & \frac{-335}{36} & 0 & 0 & 0 & 0 & 0 & 0 \end{bmatrix}, \bar{\phi}''_9(x) = \begin{bmatrix} 0 \\ 0 \\ 0 \\ 0 \\ 0 \\ 0 \\ \frac{1}{32256}\phi_{1,9}(x) \\ \frac{1}{46080}\phi_{1,10}(x) \\ \frac{1}{63360}\phi_{1,11}(x) \end{bmatrix}.$$

Again by applying four times integration to the above nine bases is as follows,

$$\int_0^x\int_0^x\int_0^x\int_0^x \phi_{1,0}(x)\,dxdxdxdx = \left[\frac{19}{1536}\quad\frac{5}{384}\quad\frac{3}{512}\quad\frac{1}{768}\quad\frac{1}{6144}\quad 0\quad 0\quad 0\quad 0\right]\phi_9(x),$$

$$\int_0^x\int_0^x\int_0^x\int_0^x \phi_{1,1}(x)\,dxdxdxdx = \left[\frac{-7}{480}\quad\frac{-7}{512}\quad\frac{-1}{192}\quad\frac{-1}{1536}\quad 0\quad\frac{1}{30720}\quad 0\quad 0\quad 0\right]\phi_9(x),$$

$$\int_0^x\int_0^x\int_0^x\int_0^x \phi_{1,2}(x)\,dxdxdxdx = \left[\frac{-1}{1152}\quad\frac{-1}{320}\quad\frac{-1}{512}\quad\frac{-1}{1152}\quad 0\quad 0\quad\frac{1}{92160}\quad 0\quad 0\right]\phi_9(x),$$

$$\int_0^x\int_0^x\int_0^x\int_0^x \phi_{1,3}(x)\,dxdxdxdx = \left[\frac{17}{336}\quad\frac{19}{384}\quad\frac{3}{160}\quad\frac{5}{1536}\quad 0\quad 0\quad 0\quad\frac{1}{215040}\quad 0\right]\phi_9(x),$$

$$\int_0^x\int_0^x\int_0^x\int_0^x \phi_{1,4}(x)\,dxdxdxdx = \left[\frac{-55}{768}\quad\frac{-13}{224}\quad\frac{-7}{384}\quad\frac{-1}{960}\quad 0\quad 0\quad 0\quad 0\quad\frac{1}{430080}\right]\phi_9(x),$$

$$\int_0^x\int_0^x\int_0^x\int_0^x \phi_{1,5}(x)\,dxdxdxdx = \left[\frac{-53}{216}\quad\frac{-65}{256}\quad\frac{-11}{112}\quad\frac{-23}{1152}\quad 0\quad 0\quad 0\quad 0\quad 0\right]\phi_9(x) + \frac{1}{774144}\phi_{1,9}(x),$$

$$\int_0^x\int_0^x\int_0^x\int_0^x \phi_{1,6}(x)\,dxdxdxdx = \left[\frac{497}{480}\quad\frac{133}{144}\quad\frac{81}{256}\quad\frac{29}{672}\quad 0\quad 0\quad 0\quad 0\quad 0\right]\phi_9(x) + \frac{1}{1290240}\phi_{1,10}(x),$$

$$\int_0^x\int_0^x\int_0^x\int_0^x \phi_{1,7}(x)\,dxdxdxdx = \left[\frac{127}{132}\quad\frac{193}{160}\quad\frac{37}{72}\quad\frac{103}{768}\quad 0\quad 0\quad 0\quad 0\quad 0\right]\phi_9(x) + \frac{1}{2027520}\phi_{1,11}(x),$$

$$\int_0^x\int_0^x\int_0^x\int_0^x \phi_{1,8}(x)\,dxdxdxdx = \left[\begin{array}{ccccccccc} \frac{-4277}{288} & \frac{-1211}{88} & \frac{-773}{160} & \frac{-335}{432} & 0 & 0 & 0 & 0 & 0 \end{array}\right]\phi_9(x) + \frac{1}{3041280}\phi_{1,12}(x),$$

Hence,

$$\int_0^x\int_0^x\int_0^x\int_0^x \phi(x)\,dxdxdxdx = H'''_{9\times 9}\ \phi_9(x) + \bar{\phi}'''_9(x),$$

where

$$H'''_{9\times 9} = \left[\begin{array}{ccccccccc} \frac{19}{1536} & \frac{5}{384} & \frac{3}{512} & \frac{1}{768} & \frac{1}{6144} & 0 & 0 & 0 & 0 \\ \frac{-7}{480} & \frac{-7}{512} & \frac{-1}{192} & \frac{-1}{1536} & 0 & \frac{1}{30720} & 0 & 0 & 0 \\ \frac{-1}{1152} & \frac{-1}{320} & \frac{-1}{512} & \frac{-1}{1152} & 0 & 0 & \frac{1}{92160} & 0 & 0 \\ \frac{17}{336} & \frac{19}{384} & \frac{3}{160} & \frac{5}{1536} & 0 & 0 & 0 & \frac{1}{215040} & 0 \\ \frac{-55}{768} & \frac{-13}{224} & \frac{-7}{384} & \frac{-1}{960} & 0 & 0 & 0 & 0 & \frac{1}{430080} \\ \frac{-53}{216} & \frac{-65}{256} & \frac{-11}{112} & \frac{-23}{1152} & 0 & 0 & 0 & 0 & 0 \\ \frac{497}{480} & \frac{133}{144} & \frac{81}{256} & \frac{29}{672} & 0 & 0 & 0 & 0 & 0 \\ \frac{127}{132} & \frac{193}{160} & \frac{37}{72} & \frac{103}{768} & 0 & 0 & 0 & 0 & 0 \\ \frac{-4277}{288} & \frac{-1211}{88} & \frac{-773}{160} & \frac{-335}{432} & 0 & 0 & 0 & 0 & 0 \end{array}\right], \bar{\phi}'''_9(x) = \left[\begin{array}{c} 0 \\ 0 \\ 0 \\ 0 \\ 0 \\ \frac{1}{774144}\phi_{1,9}(x) \\ \frac{1}{1290240}\phi_{1,10}(x) \\ \frac{1}{2027520}\phi_{1,11}(x) \\ \frac{1}{3041280}\phi_{1,12}(x) \end{array}\right].$$

4. Methodology

4.1 Differential transformation method (DTM)

Let us consider the values $\mathrm{N}=1$ and $m=0$, assuming that we have valid DTM equations (7) and (8). When we apply a differential transformation to these equations, the resulting form can be expressed as follows:

$$\begin{aligned} &(k+1)(k+2)(k+3)(k+4)F(k+4) - M^2(k+1)(k+2)F(k+2) - \\ &S\left(\begin{array}{l} \sum_{t=0}^{k}\left(\delta(k-t-1)\ (t+1)(t+2)(t+3)F(t+3)\right) + \\ 3(k+1)(k+2)F(k+2) - 2\sum_{t=0}^{k}\left(F(k-t)(t+1)(t+2)(t+3)F(t+3)\right) \end{array}\right) = 0, \end{aligned} \tag{18}$$

$$(k+1)(k+2)\theta(k+2)+Pr\,Nt\sum_{t=0}^{k}(t+1)\;\theta(t+1)(k-t+1)\theta(k-t+1)+$$
$$Pr\,S\left(2\sum_{t=0}^{k}F(k-t)\;(t+1)\theta(t+1)-\sum_{t=0}^{k}\delta(k-t-1)\;(t+1)\theta(t+1)\right)=0 \quad (19)$$

Apply the boundary conditions

$$F(0)=A,\;F(1)=0,\;F(2)=a,\;F(3)=b,\theta(0)=1,\;\theta'(0)=c. \quad (20)$$

We have included additional boundary conditions in Equation (9) at point $\eta=1$ by introducing the constants a,b and c. This allows for a more comprehensive understanding of the system.

$$F(4)=\frac{aM^2+3a\,S-6b\,S\,A}{12},F(5)=\frac{3bM^2+9b\,S-2a\,M^2S\,A}{60},$$
$$\theta(2)=\frac{-c^2Nt\,Pr-2c\;Pr\,S\,A}{2}, \quad (21)$$
$$\theta(3)=\frac{c^3Nt^2Pr^2+3c^2Nt\,Pr^2S\,A+2c\,Pr^2S^2A^2}{3}.$$

Continue the technique described above and replace the values in the next series.

$$f(\eta)=F(0)+F(1)\,\eta+F(2)\,\eta^2+F(3)\,\eta^3+F(4)\,\eta^4+F(5)\,\eta^5+F(6)\,\eta^6+\cdots \quad (22)$$

$$\theta(\eta)=\theta(0)+\theta(1)\,\eta+\theta(2)\,\eta^2+\theta(3)\,\eta^3+\theta(4)\,\eta^4+\theta(5)\,\eta^5+\theta(6)\,\eta^6+\cdots \quad (23)$$

We altered the boundary conditions from Eq. (9) into Eqs. (22) and (23) at the point $\eta=1$to determine the values of a,b,c. Then

$$f(1)=\frac{1}{2},\;f'(1)=0,\;\theta(1)=0. \quad (24)$$

To obtain the values of a,b,c, we are solving the aforementioned equations. As part of this process, we can create two polynomial equations for $f(\eta)$ and $\theta(\eta)$ by substituting the estimated values into equations (22) and (23). This approach allows us to further analyze and understand the behavior of $f(\eta)$ and $\theta(\eta)$ based on the determined values of $a,b,$ and c.

4.2 Hermite wavelet method

Now, assume that

$$f^{iv}(x) = B^T \phi(x). \tag{25}$$

Integrate Eq. (25) four times concerning x, the limit from 0 to x, and we get

$$f'''(x) = f'''(0) + B^T \left[G\phi(x) + \bar{\phi}(x) \right]. \tag{26}$$

$$f''(x) = f''(0) + xf'''(0) + B^T \left[G'\phi(x) + \bar{\phi}'(x) \right]. \tag{27}$$

$$f'(x) = f'(0) + x\, f''(0) + \frac{x^2}{2}\, f'''(0) + B^T \left[G''\phi(x) + \bar{\phi}''(x) \right]. \tag{28}$$

$$f(x) = f(0) + x\, f'(0) + \frac{x^2}{2} f''(0) + \frac{x^3}{6} f'''(0) + B^T \left[G'''\phi(x) + \bar{\phi}'''(x) \right]. \tag{29}$$

Put $f(0) = A,\ f'(0) = 0$ in Eq. (29), we have

$$f(x) = A + \frac{x^2}{2} f''(0) + \frac{x^3}{6} f'''(0) + B^T \left[G'''\phi(x) + \bar{\phi}'''(x) \right]. \tag{30}$$

Put $f(1) = \frac{1}{2},\ f'(1) = 0$ in Eqs. (29), (28) and solve those equations to obtain $f'''(0)$ and $f''(0)$, then we get

$$f'''(0) = 12A - 6 + 12 B^T \left[G'''\phi(x) + \bar{\phi}'''(x) \right]_{x=1} - 6B^T \left[G''\phi(x) + \bar{\phi}''(x) \right]_{x=1}. \tag{31}$$

$$f''(0) = -\frac{1}{2}\Big(12A - 6 + 12 B^T \left[G'''\phi(x) + \bar{\phi}'''(x) \right]_{x=1} - 6B^T \left[G''\phi(x) + \bar{\phi}''(x) \right]_{x=1} - B^T \left[G''\phi(x) + \bar{\phi}''(x) \right]_{x=1}\Big). \tag{32}$$

Substituting $f'''(0)$ and $f''(0)$ in (30) we get

$$f(x)=A-\frac{x^2}{2}\begin{pmatrix}0.5\left(12A-6+12B^T\left[G'''\phi(x)+\bar{\phi}'''(x)\right]_{x=1}-6B^T\left[G''\phi(x)+\bar{\phi}''(x)\right]_{x=1}\right)\\+B^T\left[G''\phi(x)+\bar{\phi}''(x)\right]_{x=1}\end{pmatrix}$$
$$+\frac{x^3}{6}\left(12A-6+12B^T\left[G'''\phi(x)+\bar{\phi}'''(x)\right]_{x=1}-6B^T\left[G''\phi(x)+\bar{\phi}''(x)\right]_{x=1}\right) \quad .(33)$$
$$+B^T\left[G'''\phi(x)+\bar{\phi}'''(x)\right].$$

Similarly, choose

$$\theta''(x)=N^T\phi(x). \tag{34}$$

Integrate Eq. (34) twice with respect of x, whose range is 0 to x we have

$$\theta'(x)=\theta'(0)+N^T\left[G\phi(x)+\bar{\phi}(x)\right]. \tag{35}$$

$$\theta(x)=\theta(0)+x\theta'(0)+N^T\left[G'\phi(x)+\bar{\phi}'(x)\right]. \tag{36}$$

Using $\theta(1)=0$ in Eq. (36) we have

$$\theta(0)=-1-N^T\left[G'\phi(x)+\bar{\phi}'(x)\right]\Big|_{x=1}. \tag{37}$$

Put (37) in (36), and we get

$$\theta(x)=-1-N^T\left[G'\phi(x)+\bar{\phi}'(x)\right]\Big|_{x=1}+N^T\left[G'\phi(x)+\bar{\phi}'(x)\right]. \tag{38}$$

The dependent variables $f, f', f'', f''', f^{iv}, \theta, \theta', \theta''$ are replaced in the governing differential equations using the Hermite wavelet approximations. Collocation points are chosen in the domain, for example $x_i=\frac{2i-1}{2N}$, where $i=1,2,3,\cdots,N$. This results in a system of algebraic equations involving the coefficients of the Hermite wavelet series. To determine the unknown coefficients, this system of equations is solved using the Newton-Raphson technique. The Newton-Raphson method is employed to iteratively obtain numerical solutions for the coefficient values that satisfy the entire system of equations simultaneously. This provides a numerical approximation to the differential equations (7-8).

5. Results and Discussion

The DTM and HWM are applied to study the magnetohydrodynamic flow and heat transfer of a conducting viscous fluid between disks, considering suction and injection effects. The results obtained from DTM and HWM are validated by comparing them with other published studies [50]. As shown in Tables 1-6, an excellent agreement is observed. This comparison confirms the suitability of HWM over other numerical techniques for solving highly nonlinear coupled differential equations modeling such complex flow problems. The influence of five important physical parameters on the velocity and temperature fields is presented in Figures 2-18. It is noted that $f(\eta)$ denotes the axial velocity and $f'(\eta)$ represents the radial velocity based on the formulations. Overall, the study enhances the understanding of parameter impacts on the magnetohydrodynamic flow behavior between disks using accurate numerical methods.

The energy input from uniform blowing indicates it may be possible to achieve net energy savings by controlling flow rates. Figs. 2(a,b) and 3(a,b) show parameter A influences axial and vertical velocities at the disks. At the bottom disk aligned with the positive z-direction, introducing flow between disks is expected. Figs. 2(a,b) suggests vertical velocity will become zero internally due to the bottom disk's higher entrance velocity (large A). It may exceed this value as the input flow has greater energy than the top disk. Thus, after interacting with the upstream flow and stabilizing kinetic energy, the fluid's vertical velocity achieves zero. Figs. 3(a,b) demonstrate a larger A (higher axial velocity) increase in the inlet flow rate due to conservation of mass in the incompressible flow, requiring an elevated axial output flow rate. Axial velocity fluctuations at the top disk are also depicted. Similarly, the parameter S influences velocities as seen in Figs. 4(a,b) and 5(a,b), where larger S decreases vertical velocity at a given distance. The gradient velocity for various S values remains nearly constant on the top disk per Figs. 5(a,b). Figs. 6(a,b) and 7(a,b) reveal relationships between velocities and the Hartmann number.

Suction is used to control boundary layers and aims to reduce drag or channel losses. Its effect on vertical velocity $f(\eta)$ and radial velocity $f'(\eta)$ is shown in Figs. 8(a,b) and Figs. 9(a,b). Under suction, flow condenses between disks and exits the bottom disk. For larger suction parameters, output speed exceeds the bottom disk without impacting the top disk vertical flow. Magnetic molecules attach to the top disk surface, matching its velocity. Figures 8(a,b) demonstrate $f(\eta)$ is positive for smaller A values (0.1, 0.3) while a larger A relates to stronger suction, producing negative $f'(\eta)$ per mass conservation. As no slip

occurs, Figs. 9(a,b) indicate zero u velocities on both disks, with fluid movement in the z-direction. Altering parameter S does not notably impact $f(\eta)$ and $f'(\eta)$ as seen in Figs. 8(a,b) and 9(a,b).

Squeezing flow involves both extensional and shear components. However, for small gaps and low relative velocities, shear effects are considered dominant. Figs. 10(a,b) and 11(a,b) demonstrate that increasing the squeeze parameter leads to higher axial velocities and lower vertical velocities. The top disk velocity rises with increasing parameter α, since α is proportional to w. Adhering to mass conservation, hypothetical mass leaving the top must exit through the sides and bottom. Additionally, as the squeeze parameter enlarges, the location of maximum axial velocity shifts from the centre towards the bottom disk.

The Hartmann number (M) represents the ratio of electromagnetic to viscous forces. It was first introduced by Danish physicist Julius Hartmann(1881-1951) to characterize fluid flows under magnetic fields. Higher M values correspond to stronger magnetic fields, affecting flow between disks. Literature shows friction coefficient notably increases with rise M. As observed with the parameter A previously, the axial flow direction u switched from sides to center as M increased. Conversely, axial velocity becomes negative in opposing directions determined by the right-hand rule as the force is perpendicular to this velocity. As seen in Figs. 12(a,b) and 13(a,b), increasing M lowers axial fluid velocity but has no impact on the vertical component w, in line with theoretical expectations regarding the Hartmann number's role.

Fluid temperature impacts viscosity, which determines internal friction forces resisting shear flows. As a result, temperature affects flow rates. Figs. 14-15 shows increasing suction/blowing parameter A (positively) raises the temperature, whereas blowing exhibits the opposite trend as enhanced suction permits more near-disk fluid motion. Figs. 16-18 reveal the influence of other parameters. Fig. 16 shows temperature $\theta(\eta)$ decreases with rising Prandtl number Pr, which is a dimensionless number representing the ratio of momentum diffusivity to thermal diffusivity. Similarly, Fig. 17 demonstrates temperature decreases for larger squeeze parameter S values. However, Fig. 18 illustrates that increasing the thermophoresis parameter Nt, which characterizes particle deposition rates, uniformly elevates the temperature field as expected. Overall, these results provide useful insights into controlling temperature profiles through the manipulation of influential flow parameters in magnetohydrodynamic problems.

6. Conclusion

The paper applies numerical methods to solve the governing equations modeling magnetohydrodynamic flow and heat transfer between disks. The HWM and DTM are utilized to handle the highly nonlinear system of equations characterizing the electrically conducting, suction-injection viscous fluid problem. Results demonstrated the capability of HWM and DTM to accurately solve this complex flow scenario, with solutions closely matching numerical data. Parametric analyses provided useful insights into how influential factors like the squeeze number, Hartmann number, suction parameter, thermophoresis parameter, and Prandtl number impact velocities and temperature distributions. Overall, HWM proved a powerful technique for the problem, and the study enhanced the understanding of magnetohydrodynamic dynamics between disks using numerical transformation approaches.

References

1. Schulz, M. "Control theory in physics and other fields of science: concepts, tools, and applications", *Springer Science & Business Media*, 215, (2006).
2. Ivancevic, V.G. and Ivancevic, T.T. "Applied differential geometry: a modern introduction", *World Scientific* (2007).
3. Sun, H., Zhang, Y., Baleanu, D., et al. "A new collection of real-world applications of fractional calculus in science and engineering", *Communications in Nonlinear Science and Numerical Simulation*, 64, pp. 213-231 (2018). https://doi.org/10.1016/j.cnsns.2018.04.019
4. Raghunatha, K.R. and Vinod, Y. "Viscous Flow by Expanding or Shrinking the Gap with Permeable Walls Through Hermite Wavelet Method", *International Journal of Applied and Computational Mathematics*, 9(3), pp. 22 (2023). https://doi.org/10.1007/s40819-023-01502-w
5. Raghunatha, K.R. and Siddanagowdru, S.O. "Investigation of Jeffery–Hamel flow with high magnetic field and nanoparticle by DTM", *Heat Transfer*, 51(4), pp. 3562-3572 (2022). https://doi.org/10.1002/htj.22463

6. Ümit, S.A.R.P, et al. “Applications of differential transformation method to solve systems of ordinary and partial differential equations”, *BalıkesirÜniversitesi Fen BilimleriEnstitüsüDergisi*, 20(2), pp. 135-156 (2018). https://doi.org/10.25092/baunfbed.423145
7. Sheikholeslami, M., et al. “Application of differential transformation method for nanofluid flow in a semi-permeable channel considering magnetic field effect”, *International Journal for Computational Methods in Engineering Science and Mechanics*,16(4), pp. 246-255 (2015). https://doi.org/10.1080/15502287.2015.1048384
8. Shiralashetti, S.C. and Kumbinarasaiah, S. “Laguerre wavelets collocation method for the numerical solution of the Benjamina–Bona–Mohany equations”, *Journal of Taibah University for Science*, 13(1), pp. 9-15 (2019). https://doi.org/10.1080/16583655.2018.1515324
9. Shiralashetti, S. C. and Hanaji, S. I. “Taylor wavelet collocation method for Benjamin–Bona–Mahony partial differential equations”. *Results in Applied Mathematics*, *9*, 100139 (2021). https://doi.org/10.1016/j.rinam.2020.100139
10. Shiralashetti, S.C. and Kumbinarasaiah, S. “Cardinal b-spline wavelet-based numerical method for the solution of generalized Burgers–Huxley equation”, *International Journal of Applied and Computational Mathematics*, 4, pp. 1-13 (2018). https://doi.org/10.1007/s40819-018-0505-y
11. Raghunatha, K.R., Vinod, Y., Nagappanavar, S.N., et al. “Unsteady Casson fluid flow on MHD with an internal heat source”, *Journal of Taibah University for Science*, 17(1), pp. 2271691 (2023). https://doi.org/10.1080/16583655.2023.2271691
12. Shiralashetti, S.C. and Kumbinarasaiah, S. “Hermite wavelets operational matrix of integration for the numerical solution of nonlinear singular initial value problems”, *Alexandria Engineering Journal*, 57(4), pp. 2591-2600 (2018). https://doi.org/10.1016/j.aej.2017.07.014
13. Shiralashetti, S.C. and Kumbinarasaiah, S. “New generalized operational matrix of integration to solve nonlinear singular boundary value problems using Hermite wavelets”, *Arab Journal of Basic and Applied Sciences*, 26(1), pp. 385-396 (2019). https://doi.org/10.1080/25765299.2019.1646090
14. Kumbinarasaiah, S. and Raghunatha, K.R., “The applications of Hermite wavelet method to nonlinear differential equations arising in heat transfer”, *International*

Journal of Thermofluids, 9, pp. 100066 (2021). https://doi.org/10.1016/j.ijft.2021.100066

15. Srinivasa, K., et al. "Numerical solutions of the mathematical models on the digestive system and covid-19 pandemic by Hermite wavelet technique", *Symmetry*, 13, pp. 2428 (2021). https://doi.org/10.3390/sym13122428
16. Kumbinarasaiah, S., Raghunatha, K.R., Rezazadeh, M. et al. "A solution of coupled nonlinear differential equations arising in a rotating micropolar nanofluid flow system by Hermite wavelet technique", *Engineering with Computers*,38, pp. 3351-3372 (2022). https://doi.org/10.1007/s00366-021-01462-z
17. Kumbinarasaiah, S. and Raghunatha, K.R. "Numerical solution of the Jeffery–Hamel flow through the wavelet technique", *Heat Transfer*, 51, pp. 1568-1584 (2022). https://doi.org/10.1002/htj.22364
18. Raghunatha, K.R. and Kumbinarasaiah, S. "Application of Hermite Wavelet Method and Differential Transformation Method for Nonlinear Temperature Distribution in a Rectangular Moving Porous Fin", *International Journal of Applied and Computational Mathematics*, 8, pp. 1-20 (2022). https://doi.org/10.1007/s40819-021-01226-9
19. Faheem, M., Khan, A. and Raza, A, et al. "A high-resolution Hermite wavelet technique for solving space–time-fractional partial differential equations", *Mathematics and Computers in Simulation*, 194, pp. 588-609 (2022). https://doi.org/10.1016/j.matcom.2021.12.012
20. Vinod, Y. and Raghunatha, K.R. "Application of Hermite wavelet method for heat transfer in a porous media", *Heat Transferer*, 52(1), pp. 983-999 (2023). https://doi.org/10.1002/htj.22726
21. Kumar, S., Kumar, R., Momani, S., et al. "A study on fractional COVID- 19 disease model by using Hermite wavelets", *Mathematical Methods in the Applied Sciences*, 46(7), pp. 7671-7687 (2023). https://doi.org/10.1002/mma.7065
22. Leal, L.G. "Particle motions in a viscous fluid", *Annual Review of Fluid Mechanics*, 12(1), pp. 435-476 (1980). https://doi.org/10.1146/annurev.fl.12.010180.002251
23. MacCormack, R.W. "A numerical method for solving the equations of compressible viscous flow", *AIAA Journal*, 20(9), pp. 1275-1281(1982). https://doi.org/10.2514/3.51188

24. Jalili, B., Roshani, H., Jalili, P., et al. "The magnetohydrodynamic flow of viscous fluid and heat transfer examination between permeable disks by AGM and FEM", *Case Studies in Thermal Engineering*, 45, pp. 102961 (2023). https://doi.org/10.1016/j.csite.2023.102961

25. Zhang, L., et al. "Study of nonlinear quadratic convection on magnetized viscous fluid flow over a non-Darcian circular elastic surface via spectral approach", *Journal of Taibah University for Science*, 17(1), pp. 2183702 (2023). https://doi.org/10.1080/16583655.2023.2183702

26. Zaturska, M.B., et al. "On the flow of a viscous fluid driven along a channel by suction at porous walls", *Fluid Dynamics Research*, 4(3), pp. 151 (1988). https://doi.org/10.1016/0169-5983(88)90021-4

27. Attia, H.A. "The effect of suction and injection on the unsteady flow between two parallel plates with variable properties", *Journal of Applied Science and Engineering*, 8(1), pp. 17-22 (2005). https://doi.org/10.6180/jase.2005.8.1.03

28. Mahmood, M., Hossain, M.A., Asghar, S., et al. "Application of homotopy perturbation method to deformable channel with wall suction and injection in a porous medium", *International Journal of Nonlinear Sciences and Numerical Simulation*, 9(2), pp. 195-206 (2008). https://doi.org/10.1515/IJNSNS.2008.9.2.195

29. Yuan, S.W. and Finkelstein, A.B. "Laminar pipe flow with injection and suction through a porous wall", *Transactions of the American Society of Mechanical Engineers*, *78*(4), pp. 719-724 (1956). https://doi.org/10.1115/1.4013794

30. Abdollahi, S.A., Alizadeh, A.A., Zarinfar, M., et al. "Investigating heat transfer and fluid flow betwixt parallel surfaces under the influence of hybrid nanofluid suction and injection with numerical analytical technique", *Alexandria Engineering Journal*, 70, pp. 423-439 (2023). https://doi.org/10.1016/j.aej.2023.02.040

31. Fardi, M. and Khan, Y. "Numerical simulation of squeezing Cu–Water nanofluid flow by a kernel-based method", *International Journal of Modeling, Simulation, and Scientific Computing*, 13(01), pp. 2250005 (2022). https://doi.org/10.1142/S1793962322500052

32. Fardi, M. and Machado, J.T. "Reproducing Kernel Method to Detect the Temperature Distribution for Annular Fins with Temperature-Dependent Thermal

Conductivity. *Journal of Applied Nonlinear Dynamics*, 11(02), pp. 283-295 (2022). https://doi.org/10.5890/JAND.2022.06.002

33. Ahmad, S., Ullah, H., Hayat, T., et al. "Computational analysis of time-dependent viscous fluid flow and heat transfer", *International Journal of Modern Physics B*, 34(13), pp. 2050141 (2020). https://doi.org/10.1142/S0217979220501416
34. Žukauskas, A. "Enhancement of forced convection heat transfer in viscous fluid flows", *International journal of heat and mass transfer*, 37, pp. 207-212 (1994). https://doi.org/10.1016/0017-9310(94)90022-1
35. Ismail, M., et al. "Numerical investigation on heat transfer and fluid flow behaviors of viscous fluids in a minichannel heat exchanger", *Numerical Heat Transfer Part A Applications*, 64(1), pp. 1-29 (2013). https://doi.org/10.1080/10407782.2013.773803
36. Rosenberg, D.E. and Hellums, J.D. "Flow development and heat transfer in variable-viscosity fluids", *Industrial & Engineering Chemistry Fundamentals*, 4(4), pp. 417-422 (1965). https://doi.org/10.1021/i160016a010
37. Bathe, K.J. and Dong, J. "Solution of incompressible viscous fluid flow with heat transfer using ADINA-F", *Computers & Structures*, 26(1-2), pp. 17-31 (1987). https://doi.org/10.1016/0045-7949(87)90233-1
38. Anwar, T., Kumam P., Khan, I., et al. "Generalized unsteady MHD natural convective flow of Jeffery model with ramped wall velocity and Newtonian heating; a Caputo-Fabrizio approach", *Chinese Journal of Physics*, 68, pp. 849-865 (2020). https://doi.org/10.1016/j.cjph.2020.10.018
39. Anwar, T., Khan, I., Kumam, P., et al. "Impacts of thermal radiation and heat consumption/generation on unsteady MHD convection flow of an Oldroyd-B fluid with ramped velocity and temperature in a generalized darcy medium", *Mathematics* 8(1), pp. 130 (2020). https://doi.org/10.3390/math8010130
40. Anwar, T., Kumam, P., Asifa, et al. "An exact analysis of radiative heat transfer and unsteady MHD convective flow of a second- grade fluid with ramped wall motion and temperature", *Heat Transfer*, 50(1), pp. 196-219 (2021). https://doi.org/10.1002/htj.21871
41. Kumam, P., Tassaddiq, A., Watthayu, W., et al. "Modeling and simulation-based investigation of unsteady MHD radiative flow of rate type fluid; a comparative fractional analysis", *Mathematics and Computers in Simulation*, 201, pp. 486-507 (2022). https://doi.org/10.1016/j.matcom.2021.02.005

42. Anwar, T., et al. “Unsteady MHD natural convection flow of Casson fluid incorporating thermal radiative flux and heat injection/suction mechanism under variable wall conditions”, *Scientific Reports*, 11(1), pp. 4275 (2021). https://doi.org/10.1038/s41598-021-83691-2

43. Sa'adAldin, A. and Qatanani, N. “On unsteady MHD flow through the porous medium between two parallel flat plates”, *An-Najah University Journal for Research-A (Natural Sciences)*, 30(1), pp. 173-186 (2015). https://doi.org/20.500.11888/2901

44. Nesliturk, A.I. and Tezer-Sezgin M. “The finite element method for MHD flow at high Hartmann numbers”, *Computer methods in applied mechanics and engineering*, 194(9-11), pp. 1201-1224 (2005). https://doi.org/10.1016/j.cma.2004.06.035

45. Guled, C.N., Tawade, J.V., Kumam, P., et al. “The heat transfer effects of MHD slip flow with suction and injection and radiation over a shrinking sheet by optimal homotopy analysis method”, *Results in Engineering*, 18, pp. 101173 (2023). https://doi.org/10.1016/j.rineng.2023.101173

46. Akbar, N.S., Akhtar, S., Maraj, E.N, et al. “Heat transfer analysis of MHD viscous fluid in a ciliated tube with entropy generation”, *Mathematical Methods in the Applied Sciences*, 46(10), pp. 11495-11508 (2023). https://doi.org/10.1002/mma.7906

47. Shah, N.A., Ebaid, A., Oreyeni T., et al. “MHD and porous effects on free convection flow of viscous fluid between vertical parallel plates: advance thermal analysis”, *Waves in Random and Complex Media*, pp. 1-13 (2023). https://doi.org/10.1080/17455030.2023.2186717

48. Bhargavi, N., et al. “Magnetohydrodynamic conjugate heat transfer analysis on a viscous fluid past a vertical permeable plate”, *International Journal of Modern Physics B*, pp. 2450211 (2023). https://doi.org/10.1142/S0217979224502114

49. Raghunatha, K.R. and Vinod, Y. “Effects of heat transfer on MHD suction–injection model of viscous fluid flow through differential transformation and Bernoulli wavelet techniques”, *Heat Transfer*, *52*(7), pp. 4914-4945 (2023). https://doi.org/10.1002/htj.22911

50. Fardi, M., Pishkar, I., Alidousti, J., et al. “Numerical investigation of the MHD suction–injection model of viscous fluid using a kernel-based method”, *Archive of*

Applied Mechanics, 91(10), pp. 4205-4221, (2021). https://doi.org/10.1007/s00419-021-02003-2

51. Zhou J.K. "Differential Transformation and Its Applications for Electrical Circuits", (1986).
52. Vinod, Y., et al. "Application of differential transformation and Hermite wavelet methods for micropolar flow through a permeable channel", *Heat Transfer*, 52, pp. 3094- 3118 (2023) https://doi.org/10.1002/htj.22818
53. Joneidi, A.A., et al. "Differential transformation method to determine fin efficiency of convective straight fins with temperature-dependent thermal conductivity", *International Communications in Heat and Mass Transfer*, 36, pp. 757-762 (2009). https://doi.org/10.1016/j.icheatmasstransfer.2009.03.020

Table 1 Approximation of $f''(1)$ with $(M, A) = (0.2, 0.1)$

S	Fardiet al.[50]	DTM	HWM
0.01	-2.402387733	-2.402387733	-2.402387733
0.02	-2.403175868	-2.403175868	-2.403175868
0.2	-2.417351603	-2.417351603	-2.417351603
0.25	-2.421285462	-2.421285462	-2.421285462
0.3	-2.425217671	-2.425217671	-2.425217671
0.35	-2.429148007	-2.429148007	-2.429148007

Table 2 Approximation of $f''(1)$ with $(M, S) = (0.2, 0.1)$

A	Fardiet al.[50]	DTM	HWM
-0.2	-4.232066561	-4.232066561	-4.232066561
-0.1	-3.623059453	-3.623059453	-3.623059453
0	-3.015530792	-3.015530792	-3.015530792
0.1	-2.409478752	-2.409478752	-2.409478752
0.2	-1.804901490	-1.804901490	-1.804901490
0.3	-1.201797195	-1.201797195	-1.201797195
0.4	-0.600163987	-0.600163987	-0.600163987

Table 3 Approximation of $f''(1)$ with $(S, A) = (0.1, 0.1)$

M	Fardiet al.[50]	DTM	HWM
0.01	-2.407886713	-2.407886713	-2.407886713
0.1	-2.408281818	-2.408281818	-2.408281818
0.2	-2.409478750	-2.409478750	-2.409478750
0.3	-2.411472496	-2.411472496	-2.411472496
0.4	-2.414261347	-2.414261347	-2.414261347
0.5	-2.417842954	-2.417842954	-2.417842954

Table 4 Injection flow $\left(f''(1) \right)$ results with Fardiet al. [50]

$(M,S)=(0.5,0.01)$				$(M,A)=(0.5,-1)$			
A	Fardi et al. [50]	DTM	HWM	S	Fardi et al. [50]	DTM	HWM
-0.01	-3.0741434	-3.0741434	-3.0741434	0.015	-9.0601042	-9.0601042	-9.0601042
-0.1	-3.6170373	-3.6170373	-3.6170373	0.1	-9.1882113	-9.1882113	-9.1882113
-0.2	-4.2203929	-4.2203929	-4.2203929	0.2	-9.3381070	-9.3381070	-9.3381070
-0.3	-4.8238961	-4.8238961	-4.8238961	0.3	-9.4870729	-9.4870729	-9.4870729
-0.7	-7.2393839	-7.2393839	-7.2393839	0.4	-9.6350661	-9.6350661	-9.6350661
-1	-9.0525493	-9.0525493	-9.0525493	0.5	-9.7820529	-9.7820529	-9.7820529

Table 5 Suction flow $\left(f''(1) \right)$ results with Fardiet al. [50]

$(M,S)=(0.5,0.01)$				$(S,A)=(0.4,1)$			
A	Fardiet al.[50]	DTM	HWM	M	Fardiet al.[50]	DTM	HWM
0.01	-2.95351650	-2.95351650	-2.95351650	0.1	2.91247968	2.91247968	2.91247968
0.1	-2.41076854	-2.41076854	-2.41076854	0.4	2.92042584	2.92042584	2.92042584
0.2	-1.80785529	-1.80785529	-1.80785529	1	2.96455531	2.96455531	2.96455531
0.3	-1.20508946	-1.20508946	-1.20508946	1.2	2.98742604	2.98742604	2.98742604
0.7	1.20450001	1.20450001	1.20450001	1.5	3.02910224	3.02910224	3.02910224
1	3.01014511	3.01014511	3.01014511	2	3.11733007	3.11733007	3.11733007

Table 6 Validation of results with Fardiet al. [50]

	$A=0.1, M=0.2, S=0.1$			$A=1, M=2, S=0.4$		
η	Fardi et al. [50]	DTM	HWM	Fardi et al. [50]	DTM	HWM

0.10	0.216945117	0.216945117	0.216945117	-0.297884946	-0.297884946	-0.297884946
0.20	0.384801282	0.384801282	0.384801282	-0.505873586	-0.505873586	-0.505873586
0.40	0.575554145	0.575554145	0.575554145	-0.713542841	-0.713542841	-0.713542841
0.50	0.599174553	0.599174553	0.599174553	-0.731526711	-0.731526711	-0.731526711
0.55	0.593125400	0.593125400	0.593125400	-0.721093460	-0.721093460	-0.721093460
0.60	0.575174467	0.575174467	0.575174467	-0.697912886	-0.697912886	-0.697912886
0.65	0.545313913	0.545313913	0.545313913	-0.661889099	-0.661889099	-0.661889099
0.80	0.384040429	0.384040429	0.384040429	-0.472861417	-0.472861417	-0.472861417
0.85	0.306258048	0.306258048	0.306258048	-0.380561374	-0.380561374	-0.380561374
0.90	0.216373180	0.216373180	0.216373180	-0.271931012	-0.271931012	-0.271931012

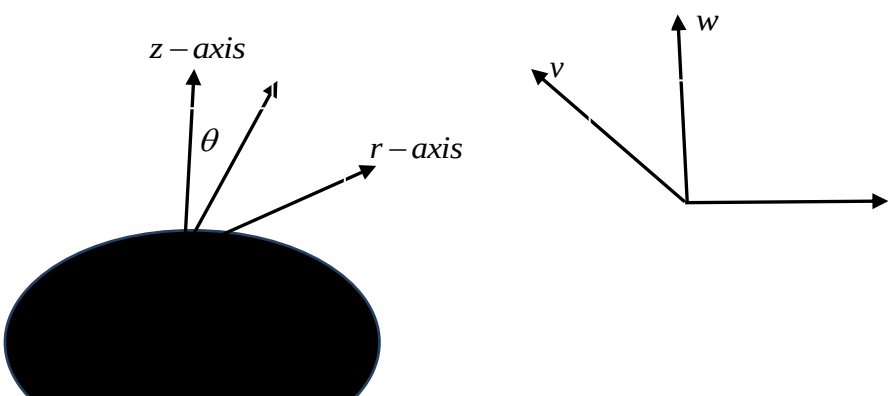

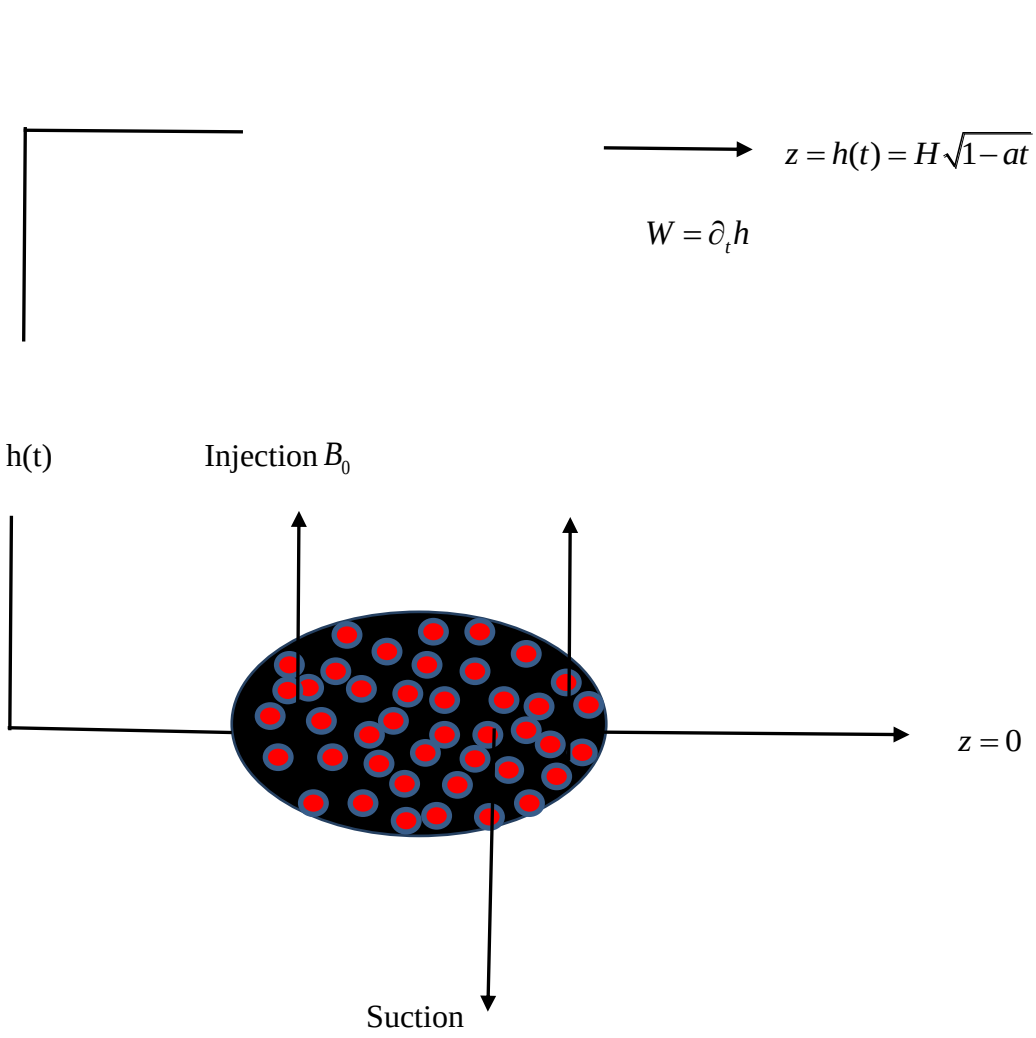

Figure 1. Physical configuration of the problem.

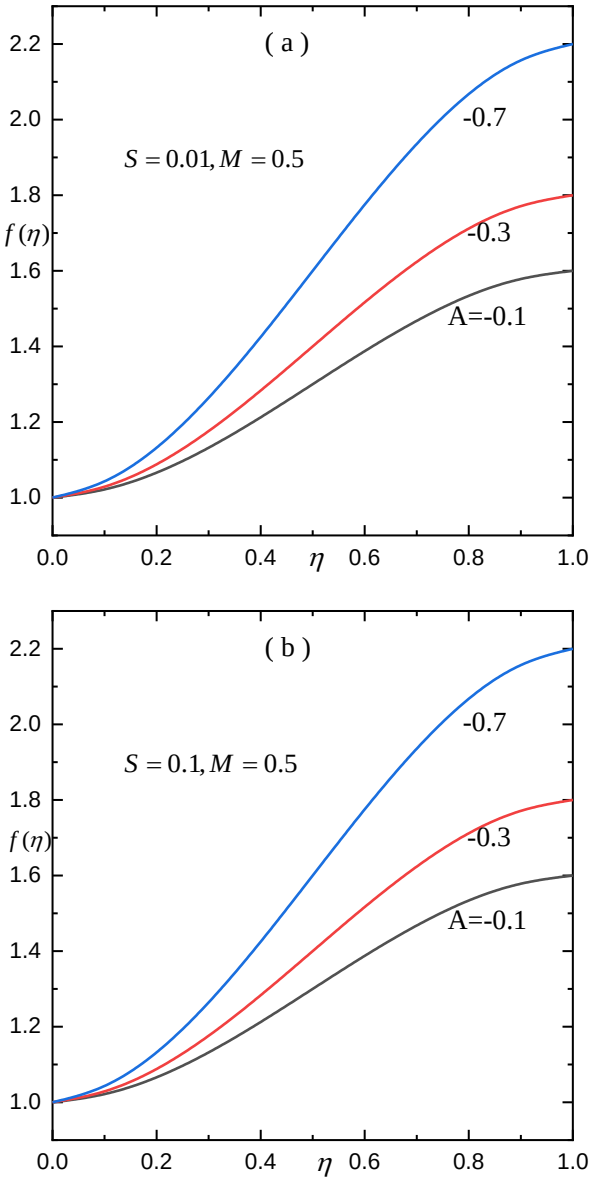

Figure 2. Influence of injection parameter on vertical velocity $f(\eta)$

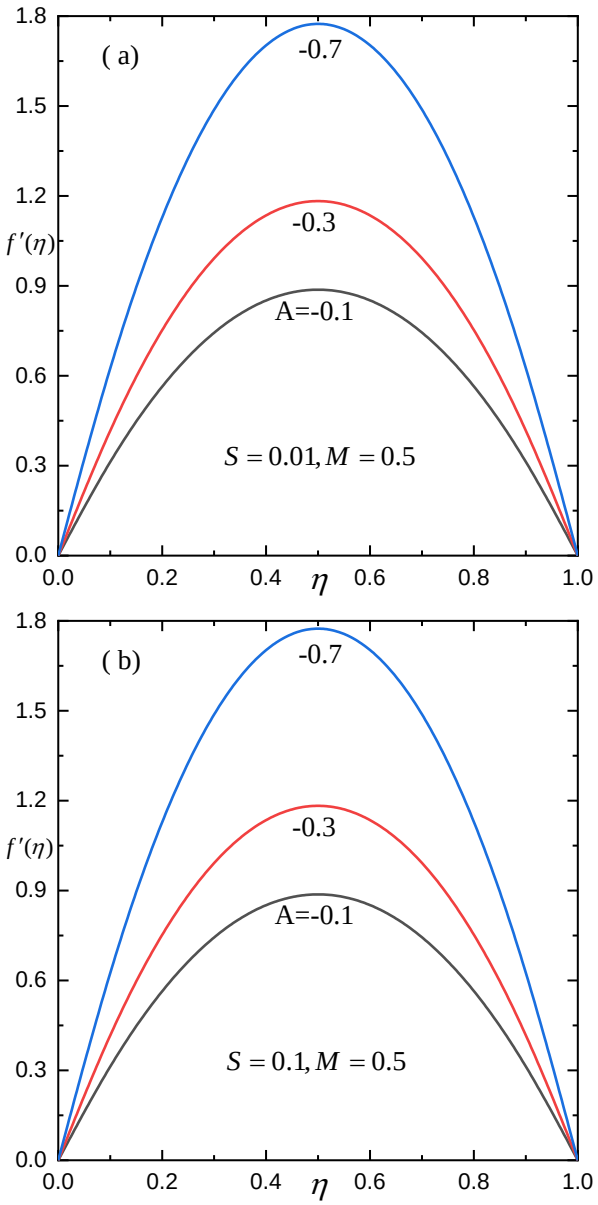

Figure 3. Influence of suction parameter on axial velocity $f'(\eta)$

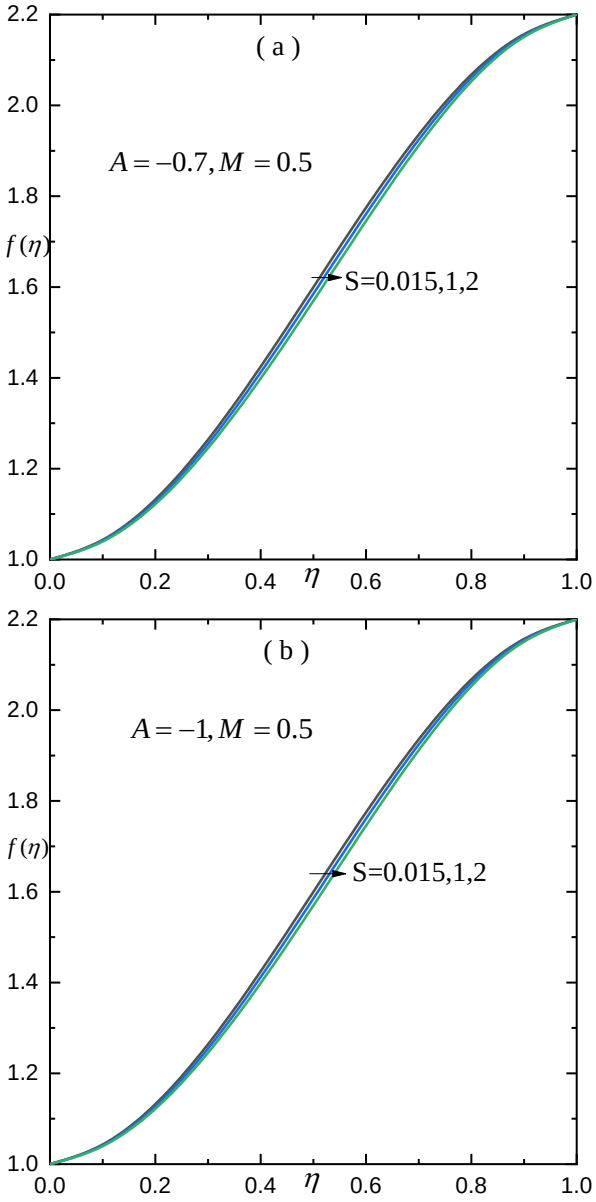

Figure 4. Influence of squeezing parameter on vertical velocity $f(\eta)$

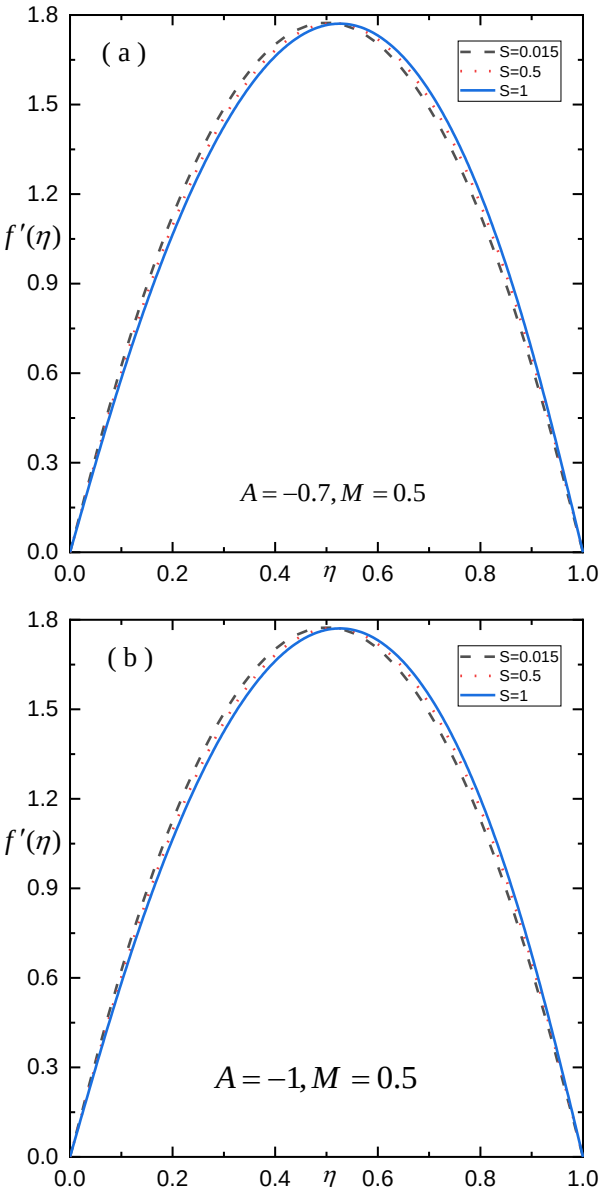

Figure 5. Influence of squeezing parameter on axial velocity $f'(\eta)$

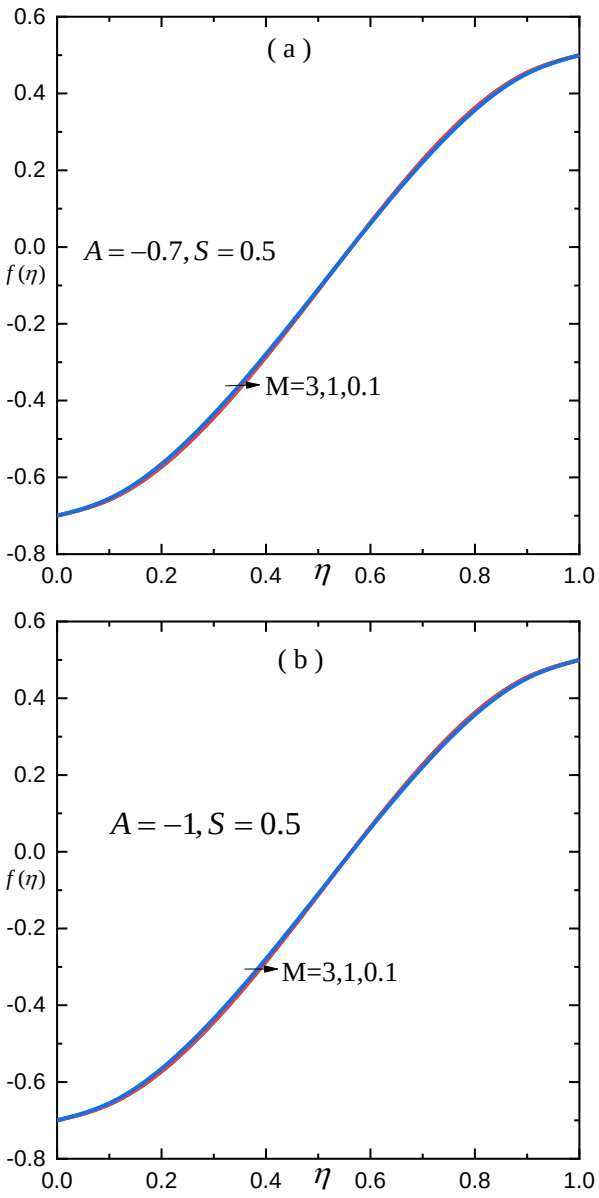

Figure 6. Influence of Hartmann number on vertical velocity $f(\eta)$

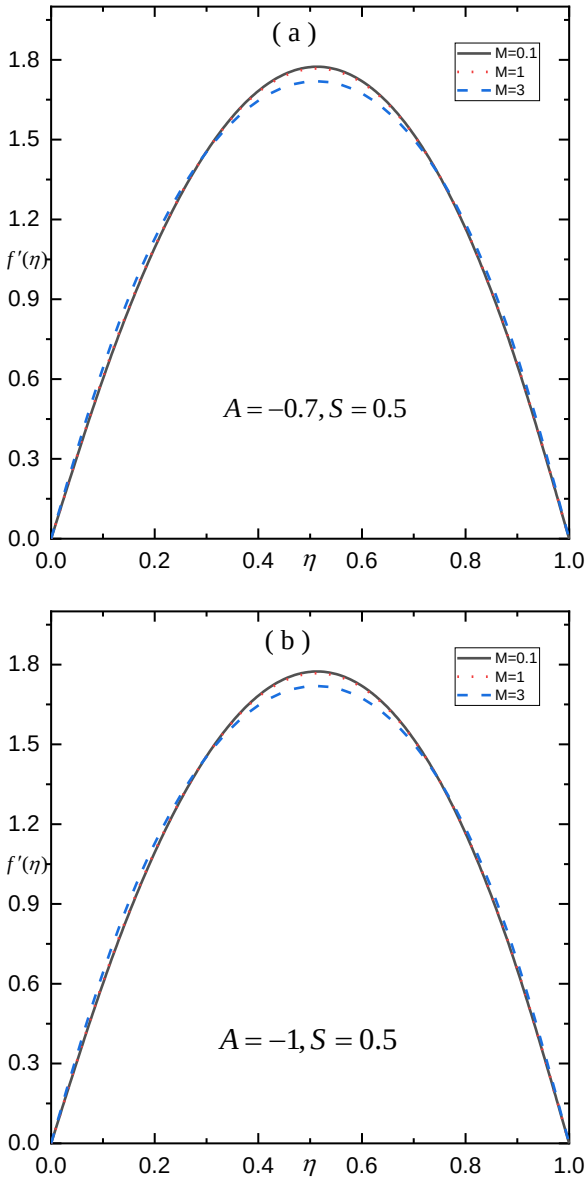

Figure 7. Influence of Hartmann number on axial velocity $f'(\eta)$

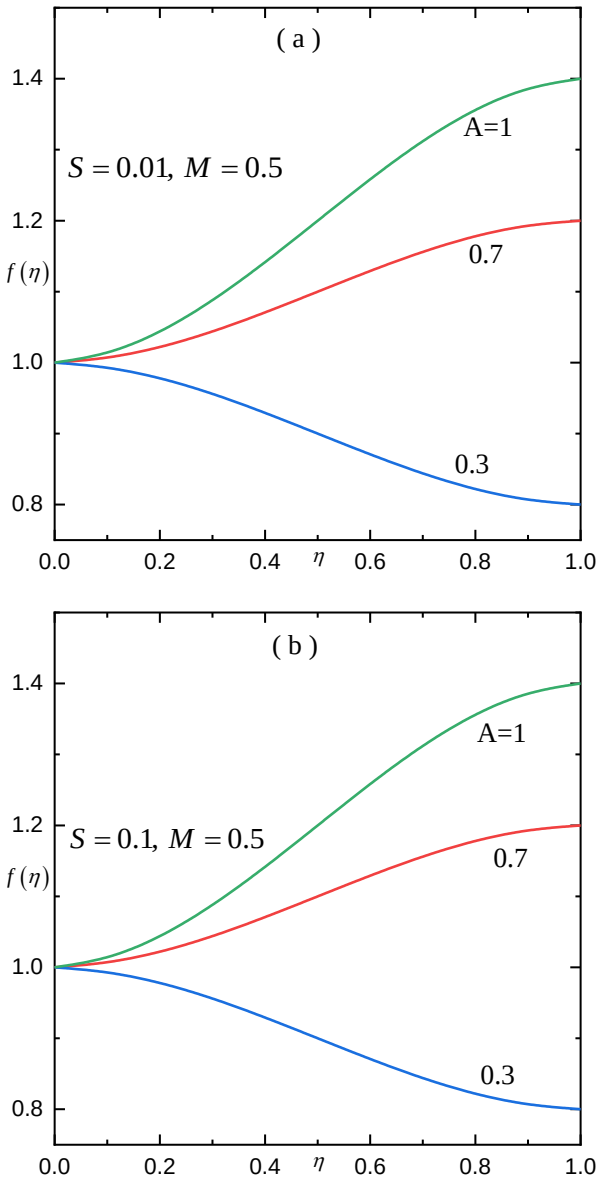

Figure 8. Influence of suction parameter on vertical velocity $f(\eta)$

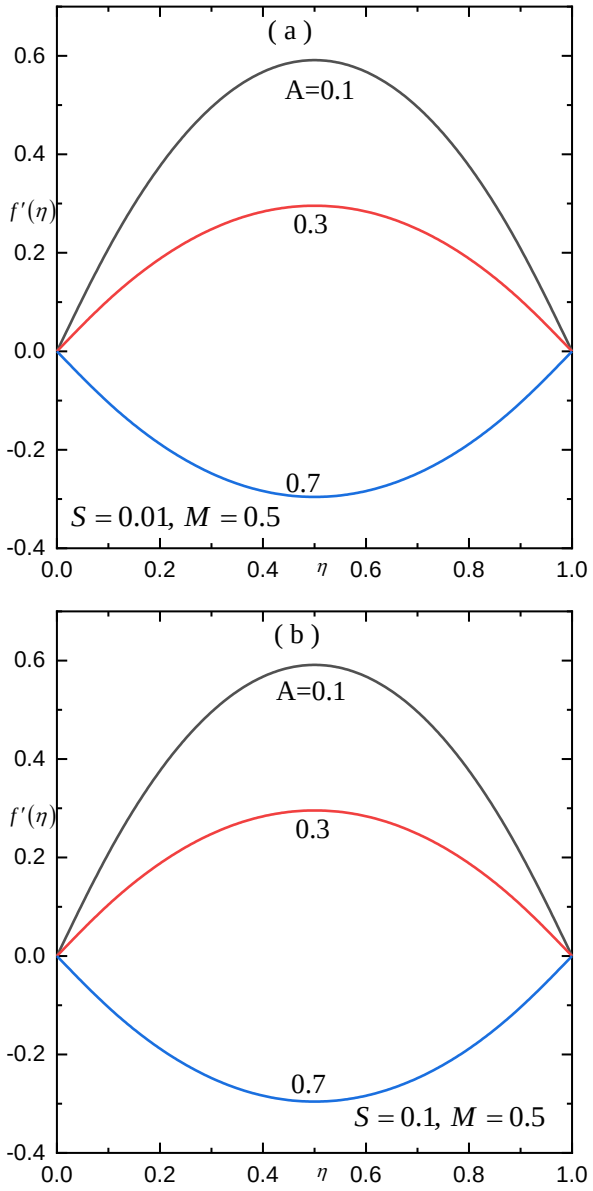

Figure 9. Influence of suction parameter on axial velocity $f'(\eta)$

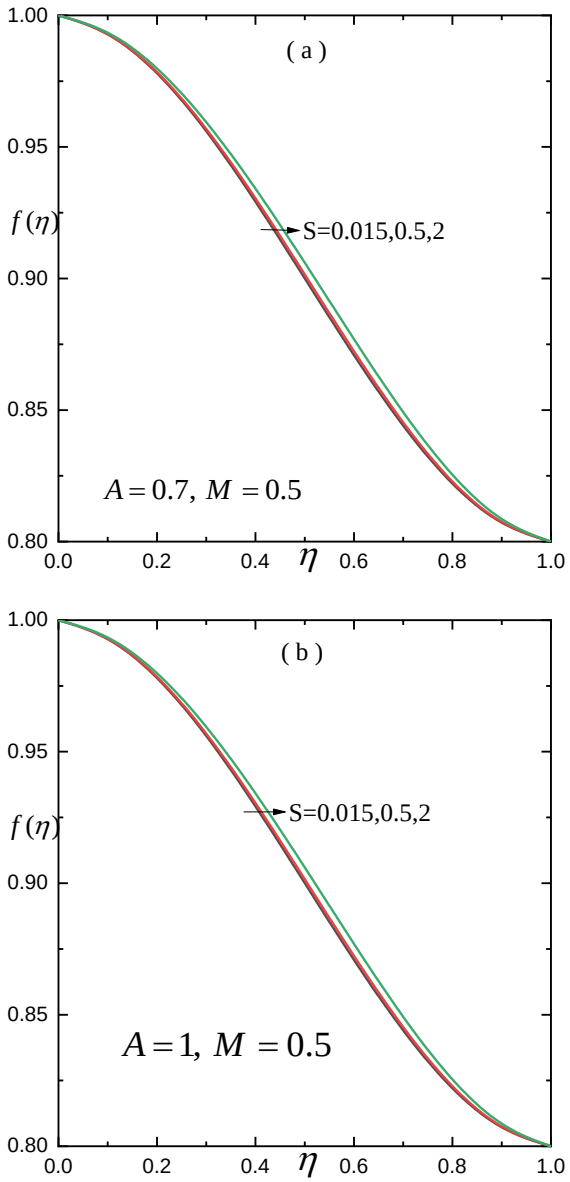

Figure 10. Influence of squeezing parameter on vertical velocity $f(\eta)$

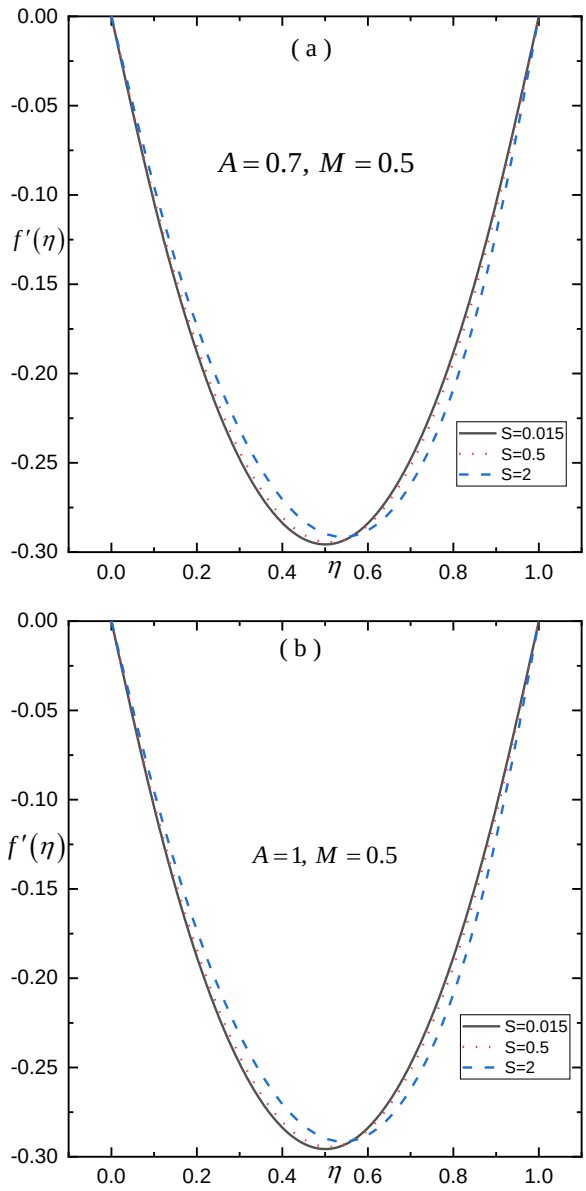

Figure 11. Influence of squeezing parameter on axial velocity $f'(\eta)$

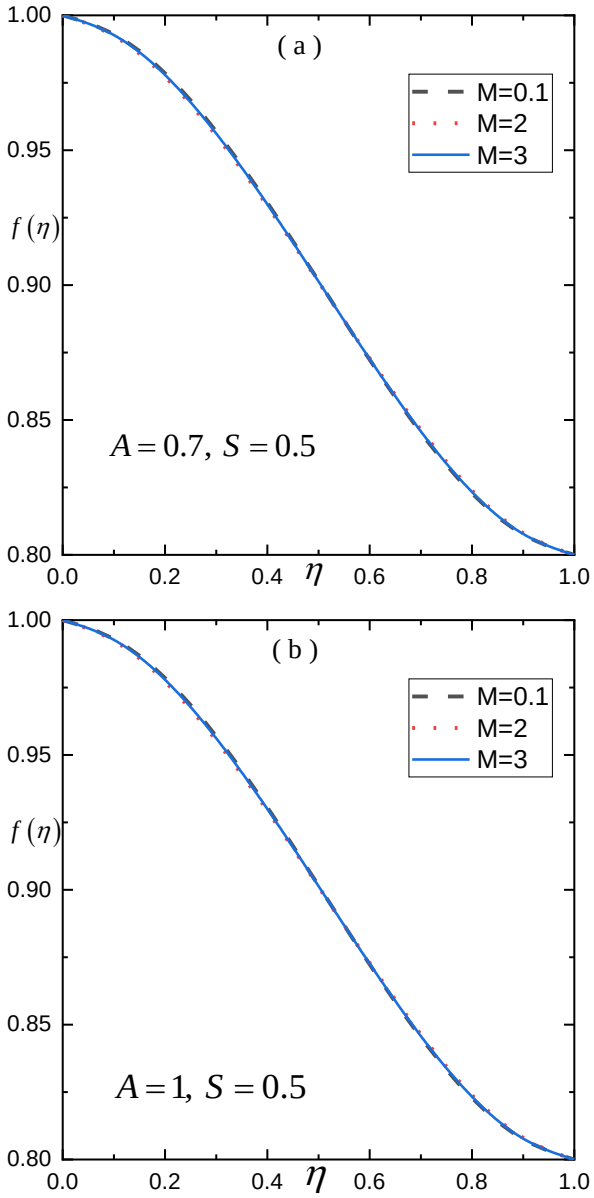

Figure 12. Influence of Hartmann number on vertical velocity $f(\eta)$

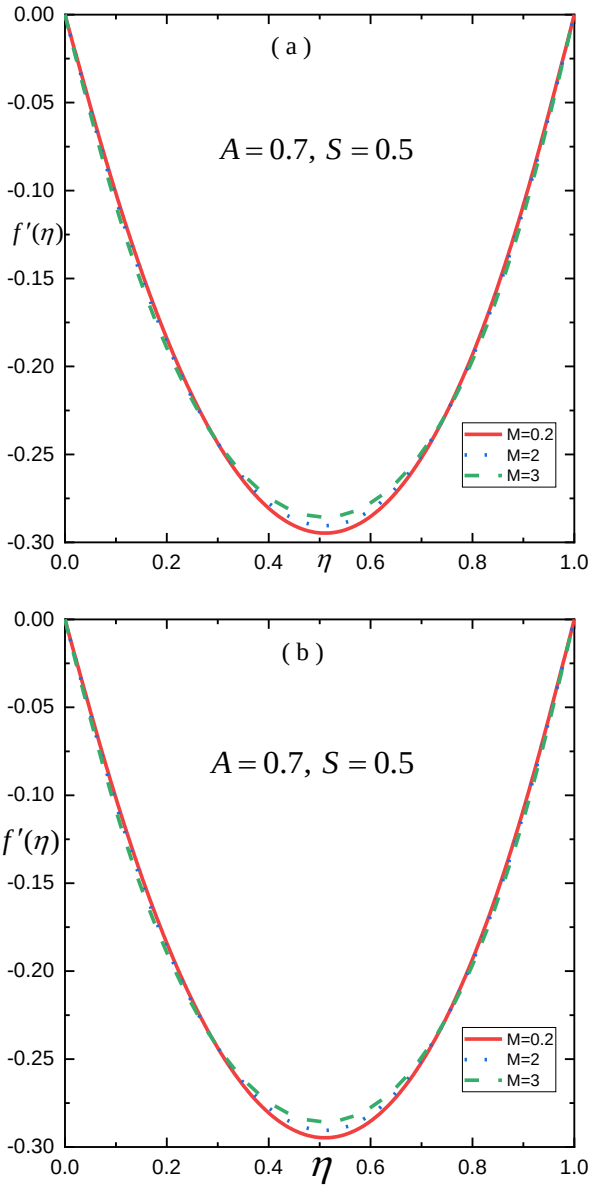

Figure 13. Influence of Hartmann number on axial velocity $f'(\eta)$

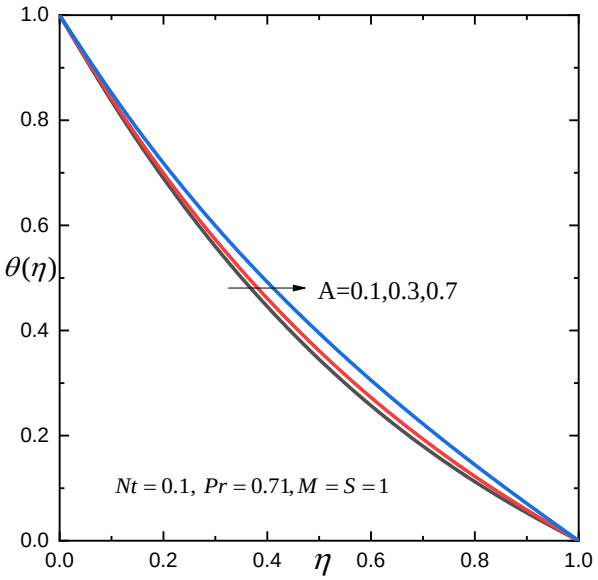

Figure 14. Influence of suction parameter on $\theta(\eta)$

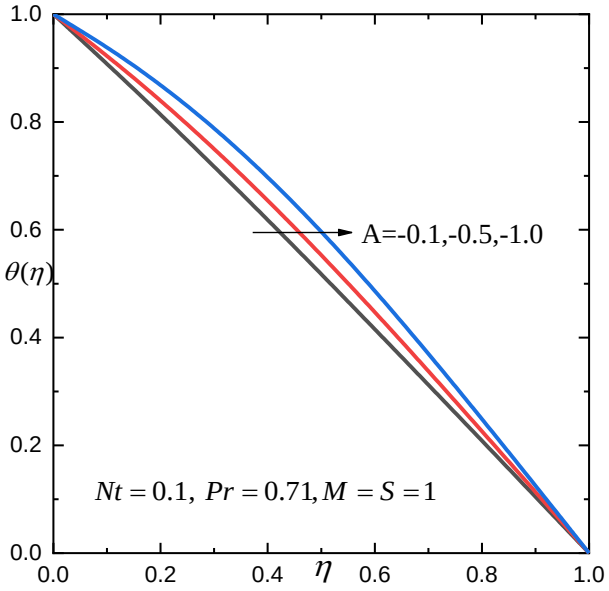

Figure 15. Influence of injection parameter on $\theta(\eta)$

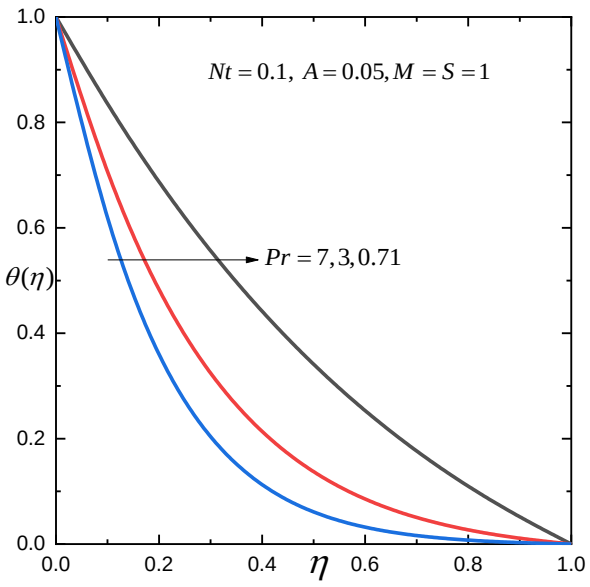

Figure 16. Influence of Prandtl number on $\theta(\eta)$

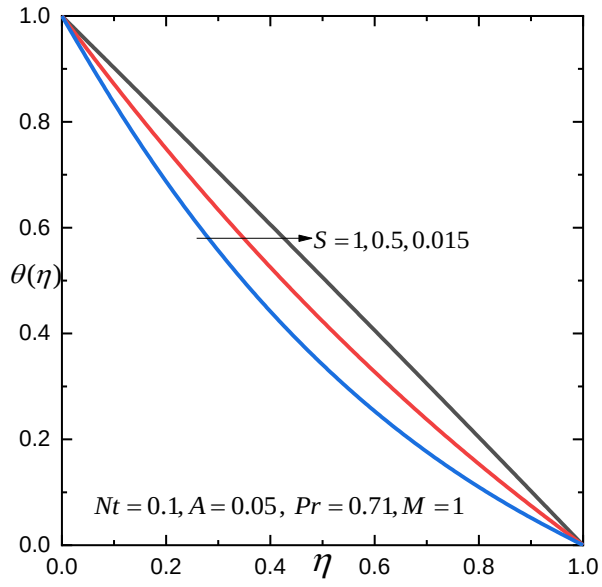

Figure 17. Influence of squeeze number on $\theta(\eta)$

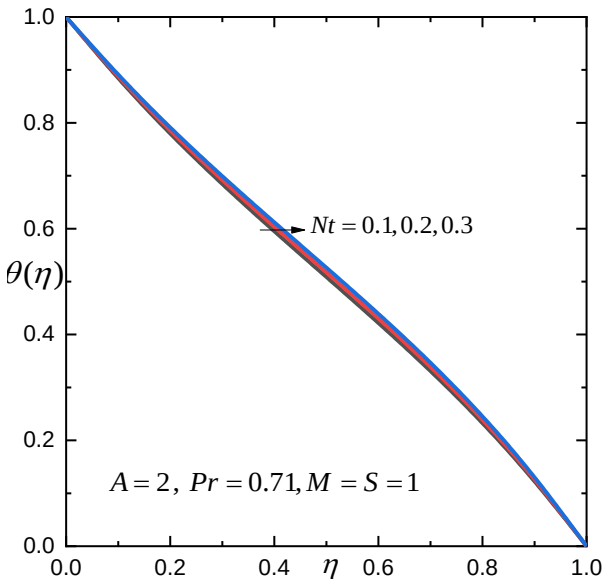

Figure 18. Influence of Thermophoresis number on $\theta(\eta)$

Author Details

K. R. Raghunatha and Vinod Y.
Department of Mathematics,
Davangere University,
Davangere- 577 007, India
e-mail: raghunatha13@gmail.com
Vinod Y.
e-mail: **vinod.vinu.vy@gmail.com**

Kumbinarasaiah S.
Department of Mathematics,
Bangalore University,
Bangalore- 560056, India
Phone no: 919663033560
Corresponding author email: kumbinarasiah@gmail.com

A brief technical biography of each author

K. R. Raghunatha received his Ph.D. degree in Mathematics from Bangalore University, Bengaluru. Currently, he is an Assistant Professor at the Department of Mathematics, Davangere University, Davangere. Dr. K. R. Raghunatha has more than six years of research and teaching experience. His main research interest is Fluid Mechanics.

Vinod Y. received his M.Sc. degree in Mathematics from Central University of Karnataka, Kalaburagi. Currently, he is a research scholar in the Department of Mathematics at Davangere University, Davangere, under the supervision of Dr. K. R. Raghunatha. His research interests include Wavelet analysis and Fluid Mechanics.

Kumbinarasaiah S. received his Ph.D. degree in Mathematics from Karnatak University, Dharwad. Currently, he is an Assistant Professor at the Department of Mathematics, Bangalore University, Bengaluru. Dr. Kumbinarasaiah S has more than ten years of research and teaching experience. His main research interests include Wavelet theory, Numerical analysis, and Fluid Mechanics.